



**Trip Report for**  
**“American Chemical Society**  
**236<sup>th</sup> National Meeting”**  
**Philadelphia, PA**  
**August 17-21, 2008**

**Xinchao Chen, Ph.D., Jinhai Yang, Ph.D., William Geiss, Ph.D.,  
Joseph Raker, Ph.D., Jason Davis, Ph.D. and Deepu Varughese**

---

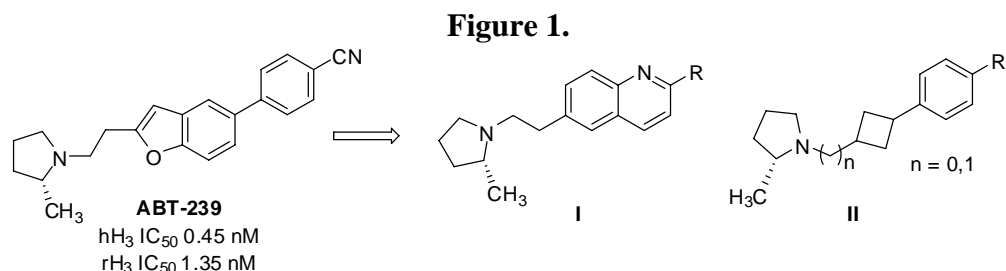
**Abstract:** *The 236<sup>th</sup> ACS National Meeting was held in Philadelphia, PA from August 17-21, 2008. The following report is a collection of summaries from oral and poster presentations attended and viewed by the contributors during the meeting.*

---

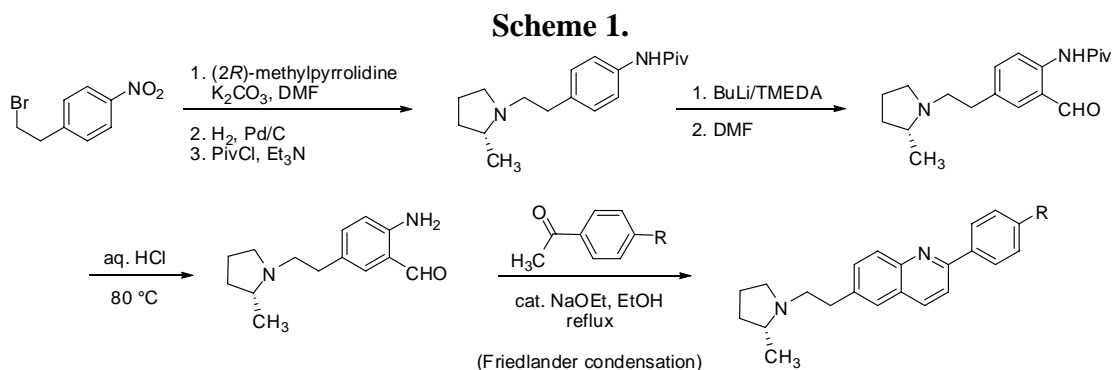
## “Discovery of Two Novel Series of Histamine H<sub>3</sub> Antagonists”

Huaqing Liu, Abbott Laboratories

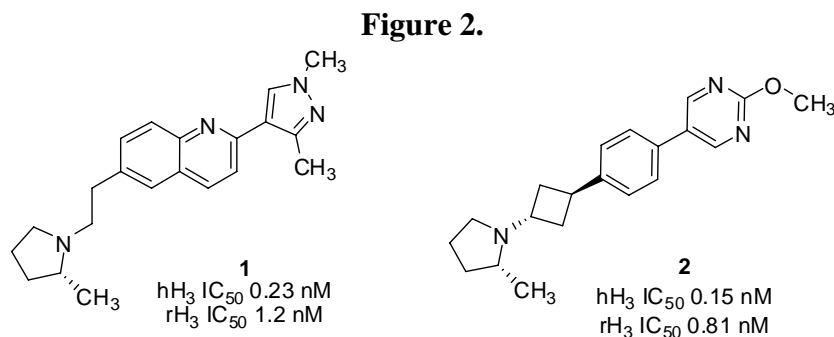
Histamine H<sub>3</sub> is one of a family of four G protein-coupled receptors mediating neurotransmitters with multiple physiological functions. These neurotransmitters play an important role in cognition, vigilance and wakefulness. The potential therapeutic utility of H<sub>3</sub> antagonists includes treatments for ADHD, Alzheimer’s disease and schizophrenia. Compounds were sought as backups for **ABT-239** which has entered clinical trials (Figure 1). Two series of analogues were designed: quinoline derivatives **I** and phenyl cyclobutanes **II**.



Typical chemistry for the synthesis of quinoline derivatives is shown in Scheme 1, and some SAR results are shown in Table 1.



Compound **1** was selected for further development from this series (Figure 2). In the other series, extensive SAR studies resulted in the selection of compound **2** for further development.

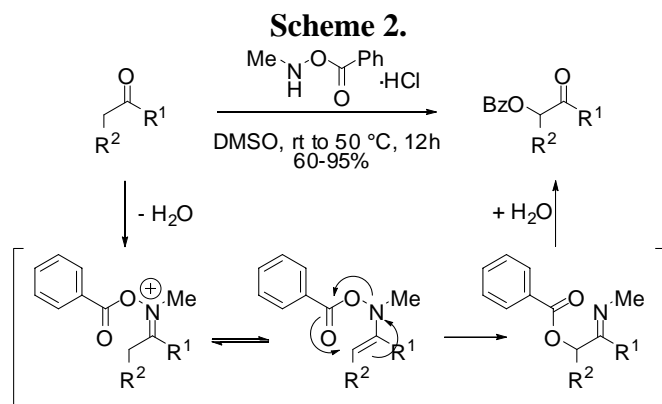


R	hH <sub>3</sub> IC <sub>50</sub> (nM)	rH <sub>3</sub> IC <sub>50</sub> (nM)	R	hH <sub>3</sub> IC <sub>50</sub> (nM)	rH <sub>3</sub> IC <sub>50</sub> (nM)	R	hH <sub>3</sub> IC <sub>50</sub> (nM)	rH <sub>3</sub> IC <sub>50</sub> (nM)
	0.34	0.62		0.42	3.7		2.7	11
	0.75	7.3		0.19	0.67		0.16	0.68
	0.11	0.5		0.23	1.0		0.23	1.2
	0.25	0.48		1.1	3.4		0.44	1.6
	0.15	0.45		0.32	1.2		0.19	1.4
	0.36	2.2		1.6	5.2		0.56	1.5
	0.22	1.9		1.6	4.6			
	0.11	.52						

### “A Practical Method for the Asymmetric $\alpha$ -Oxygenation of Carbonyl Compounds”

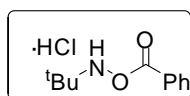
Deborah A. Knowles, Christopher J. Matthews and Nicholas C. O. Tomkinson, School of Chemistry, Cardiff University, UK

A new family of hydroxylamine reagents for the metal-free  $\alpha$ -functionalisation of carbonyl compounds have been developed as shown in Scheme 2.

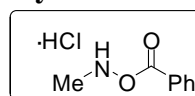


The reactions can be carried out at room temperature in the presence of moisture and air. Further development of the method led to a series of reagents based around a generic hydroxylamine scaffold providing a new family of reagents for  $\alpha$ -oxy-functionalization (Figure 3).

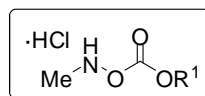
**Figure 3.  $\alpha$ -Oxybenzoylation.**



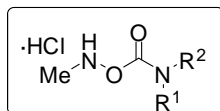
A chemo-specific reagent for the  $\alpha$ -oxybenzoylation of aldehydes. *Chem. Comm.* **2005**, 1478.



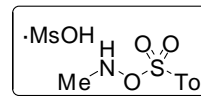
A general reagent for the  $\alpha$ -oxybenzoylation of carbonyl compounds. *Org. Lett.* **2005**, 5729; *Org. Synth.* **2007**, 233.



$\alpha$ -Oxycarbonylation  
*Synlett* **2006**, 3435.



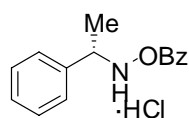
$\alpha$ -Oxycarbamoylation  
*Synlett* **2007**, 293.



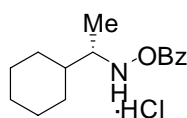
$\alpha$ -Oxysulfonylation  
*Org. Lett.* **2007**, 4009.

Further synthetic efforts have incorporated chiral amines into the structure of the reagent in order to achieve these processes asymmetrically. Reagents are prepared in one step by treatment of a primary amine with benzoyl peroxide under basic reaction conditions. A series of reagents (**1-4**, Figure 4) were synthesised using this method and were found to be stable compounds which could be stored under air for several months without apparent degradation.

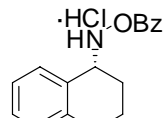
**Figure 4.**



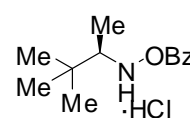
1·HCl  
67%



2·HCl  
76%



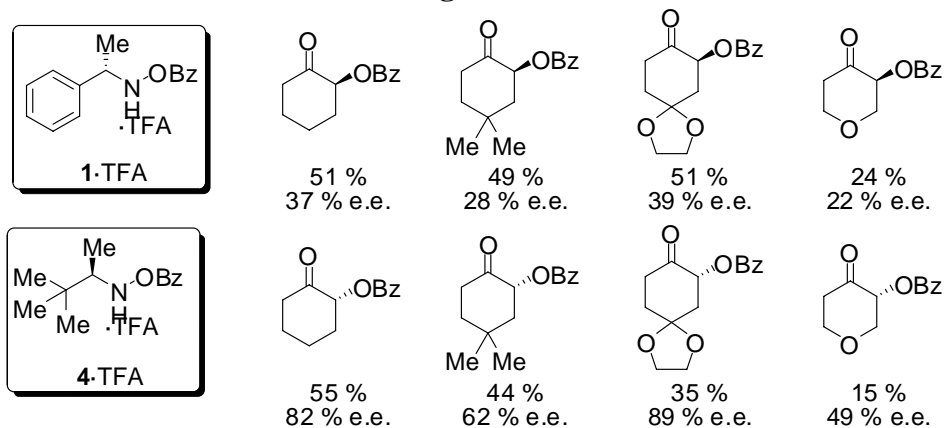
3·HCl  
45%



4·HCl  
63%

The screening of reaction conditions included variables such as solvent, co-acid, temperature, concentration, time and substrate. This extensive study revealed a number of interesting findings: use of strong co-acids provided reactive reagents but low levels of asymmetric induction; weaker co-acids such as TFA provided the optimal balance between activity and level of asymmetric induction; polar solvents such as DMSO provided good reactivity but no asymmetric induction; highest levels of asymmetric induction were obtained in non-polar aromatic solvents such as toluene; the products did not racemise under the reaction conditions; lowering of reaction temperature was beneficial to the enantioselection obtained but significantly reduced the overall reaction rate; two equivalents of reagent provided optimal reaction conditions. Moderate to good asymmetric inductions were observed with some substrates (Figure 5).

**Figure 5.**



---

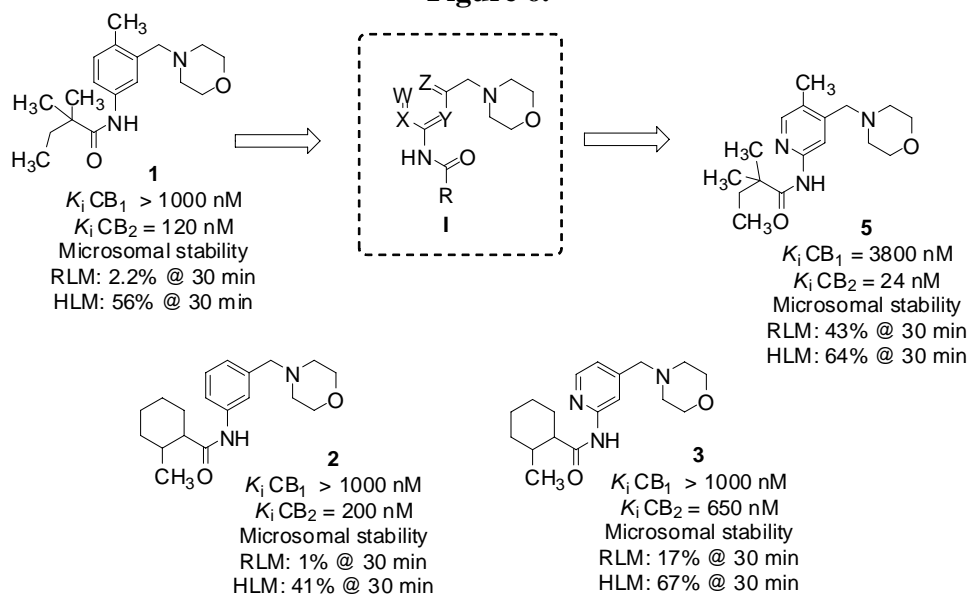
**“Novel Selective CB2 Receptor Ligands: Part VIII-Pyridine Derivatives 1”**

*Guo-Hua Chu, Christopher T. Saeui, Karin Worm, Damian G. Weaver, Allan J. Goodman, Rosalyn Green, Q. Jean Zhou, Robert L. Broadrup, Doreen-Marie S. Dulay, Bertrand Le Bourdonnec, Ian Sellitto, Christopher W. Ajello, Lara K. Leister, Heather O’Hare, Joel A. Cassel, Gabriel J. Stabley, Robert N. DeHaven, Nathalie Conway-James, Christopher LaBuda, Michael Koblisch, Patrick J. Little, Bernice L. Brogdon, Steven A. Smith and Roland E. Dolle, Adolor Corporation, PA*

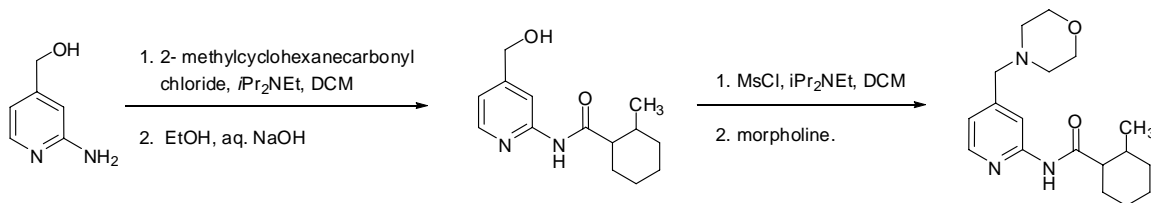
In animal models of acute and persistent nociception, cannabinoid receptor agonists significantly diminish pain responses. There are two receptor subtypes, CB1 and CB2, that mediate cannabinoid antinociception. The CB1 receptor is expressed primarily in the central nervous system (CNS), whereas the CB2 receptor is primarily expressed in peripheral tissues and is absent in the CNS. Preclinical studies have shown that CB2 cannabinoid receptor-selective agonists inhibit signs of acute nociceptive, inflammatory and neuropathic pain, and importantly they do not cause the CNS side effects typically produced by cannabinoid ligands with agonist activity at the CB1 receptor. Therefore, selective CB2 receptor agonists are very promising candidates for pain management.

Aminomethyl benzamides (compounds **1** and **2**, Figure 6) have been identified as a novel series of cannabinoid CB2 receptor ligands. However, these (morpholinomethyl)aniline amide derivatives have unfavorable PK profiles. In order to improve the metabolic stability and bioavailability of these compounds, the benzene core was replaced with a pyridine ring in order to block undesired metabolism. Typical chemistry is shown in Schemes 3 and 4. Such replacement led to the discovery of a novel chemical class of CB2 ligands with the general structure **I** (Figure 6). These compounds were shown to be highly potent and selective CB2 agonists with significantly improved metabolic stability. One representative compound, 2,2-dimethyl-*N*-(5-methyl-4-(morpholinomethyl)pyridin-2-yl)butanamide (**5**), was efficacious in *in vivo* pain assays.

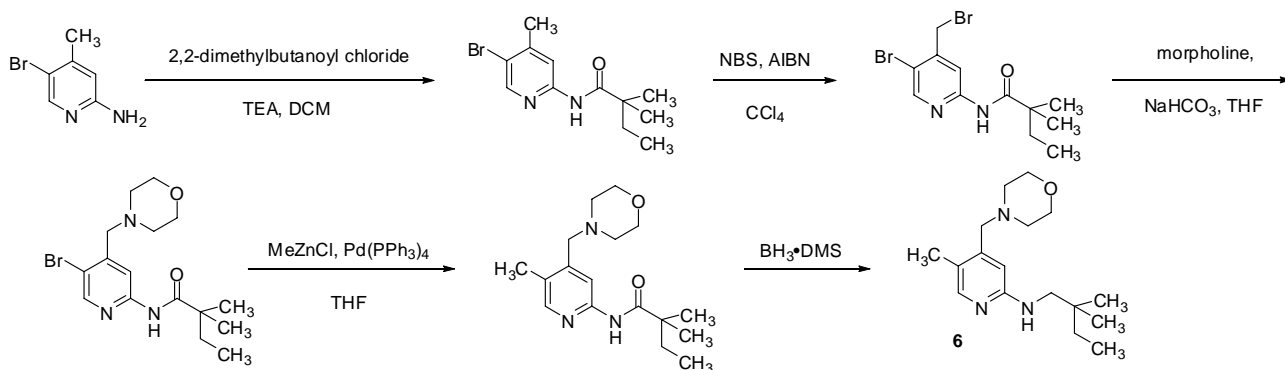
**Figure 6.**



**Scheme 3.**



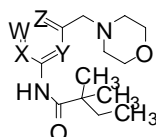
**Scheme 4.**



The *in vitro* CB receptor binding and liver microsome assay results of the pyridine derivatives **4-16** are shown in Table 2. Compound **3** exhibited a 3-fold decrease of CB<sub>2</sub> binding affinity, however with improved metabolic stability compared to its benzene analog, compound **2** (Figure 6). The 5-bromo substituted compound **4** had a very good CB<sub>2</sub> affinity with moderate metabolic stability. Conversion of the bromo to methyl led to the discovery of compound **5** which showed a 5-fold increase of CB<sub>2</sub> affinity as compared to **1**, high selectivity versus CB<sub>1</sub> (160-fold) and significantly improved metabolic stability.

Various structural modified analogs of compound **5** were prepared to explore the SAR of this new chemical class of CB2 ligands. Reduction of the amide functionality of **5** resulted in dramatic drop of the metabolic stability (compound **6**). The regiomerics analogs of compound **4** and **5**, compounds **7-13** showed significant loss of CB2 affinity, indicating the substitution pattern of the pyridine ring had significant impact on the CB2 binding affinity. Replacement of the methyl group at the 5-position in **5** with a bigger alkyl substitution group, such as ethyl (compound **14**) increased the CB2 affinity, but attenuated the metabolic stability. On the other hand, replacement of the 5-methyl with CN (compound **19**) or NH<sub>2</sub> (compound **16**) caused a significant decrease of CB2 affinity. These data suggest that the substitution group at the 5-position is important for obtaining both high CB2 binding affinity and metabolic stability, with a small alkyl group most preferred.

**Table 2.**



Cmpd	W	X	Y	Z	K <sub>i</sub> CB <sub>1</sub> [nM or % inh @ 10 mM]	K <sub>i</sub> CB <sub>2</sub> @ 10 mM]	Ratio CB <sub>1</sub> /CB <sub>2</sub>	EC <sub>50</sub> (nM)	Microsomal RLM	Stability HLM
<b>4</b>	CH	N	CH	CBr	1500	18	80	23	23	24
<b>5</b>	CH	N	CH	CCH <sub>3</sub>	3800	24	160	41	43	64
<b>6</b>	CH	N	CH	CCH <sub>3</sub>	3500	11	320	13	0	20
<b>7</b>	CH	CH	N	CBr	40%	610	nd	nd	nd	nd
<b>8</b>	CH	CH	N	CCH <sub>3</sub>	28%	1800	nd	nd	nd	nd
<b>9</b>	N	CH	CH	CBr	7%	650	nd	nd	nd	nd
<b>10</b>	N	CH	CH	CCH <sub>3</sub>	4%	46%	nd	nd	nd	nd
<b>11</b>	CCH <sub>3</sub>	CH	CH	N	8%	37%	nd	nd	nd	nd
<b>12</b>	CCH <sub>3</sub>	CH	N	CH	18%	470	nd	nd	nd	nd
<b>13</b>	CCH <sub>3</sub>	N	CH	CH	0%	67	nd	260	nd	nd
<b>14</b>	CH	N	CH	Et	4300	7.9	550	9.6	29	34
<b>15</b>	CH	N	CH	CCN	11%	100	nd	200	nd	nd
<b>16</b>	CH	N	CH	CNH <sub>2</sub>	10%	870	nd	nd	nd	nd

In summary, core replacement of phenyl with a pyridine ring led to the discovery of a novel chemical series of potent and selective CB2 ligands. In particular, compound **5**, a potent and highly selective CB2 agonist with significantly improved metabolic stability, displayed antiallodynic and antihyperalgesic activities in L5 SNL, FCA and Carrageenan models at 100 mg/kg po.

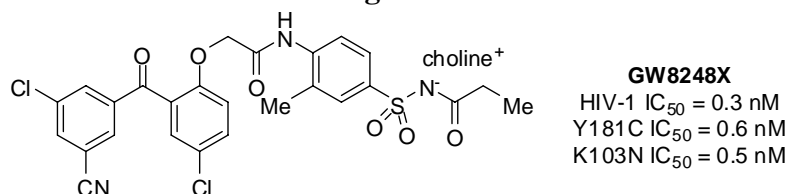
### “Lead Optimization Studies of GW 8248X, a Novel Benzophenone NNRTI for the Treatment of HIV-1”

*M. Tallant, M. Edelstein, R. Ferris, G. Freeman, P. Chong, H. Zhang, H. Marr, D. Todd, D. Lang, and M. McIntyre, GlaxoSmithKline, NC*

Benzophenone derivative **GW8248X** was selected as a non-nucleoside reverse transcriptase inhibitor (NNRTI) for the treatment of HIV-1 infection (Figure 7). It is a

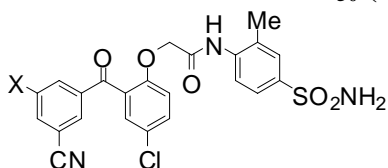
highly potent compound which has shown clinical efficacy in NNRTI-experienced patients.

**Figure 7.**



However, a study conducted in healthy volunteers showed an unexpectedly high incidence of rash. Crystallization of **8248X** in rat liver was observed in 6-month safety assessment studies at high doses, indicating poor solubility of parent drug. Due to these findings, **GW8248X** was withdrawn from clinical trials and alternative compounds were sought. The goal was to maintain “8248-like” potency against selected mutants, to increase aqueous solubility and to have an acceptable pharmacokinetic profile. Some A-ring SAR results are shown in Table 3.

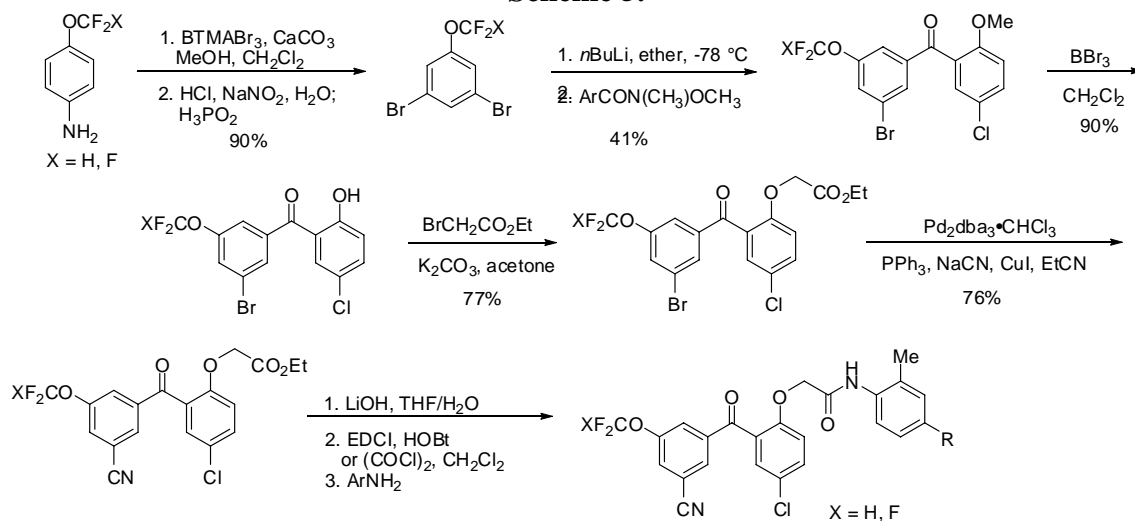
**Table 3. A-Ring Analogues Antiviral Activities IC<sub>50</sub> (nM) in HeLa Cell Assay**



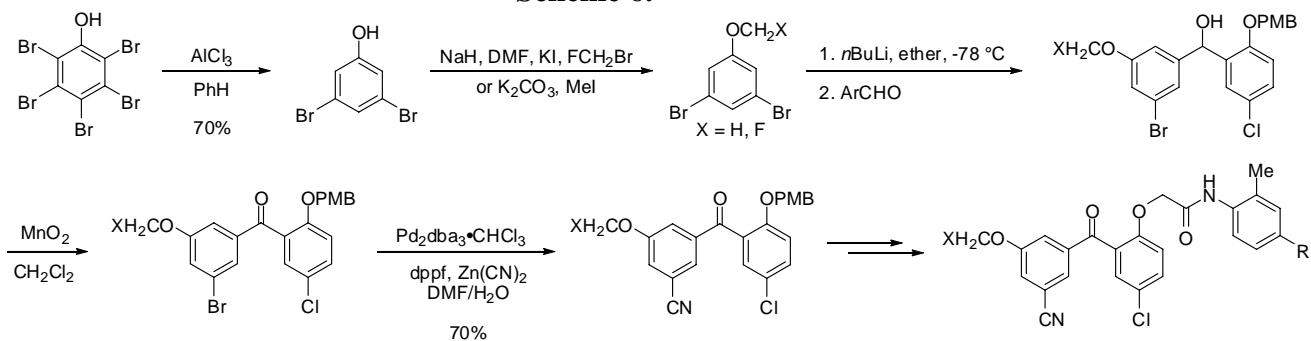
X	wtRVA	K103N	Y181C	V106A
Cl	0.4	0.7	0.7	2.3
CH <sub>2</sub> OH	2.0	4.5	6.4	67.0
CH <sub>3</sub> CO	0.7	1.3	1.9	21.0
CO <sub>2</sub> H	930	1300	>2000	>2000
CH <sub>3</sub> NHCO	445	980	>2000	>2000
CO <sub>2</sub> Me	0.9	1.4	2.9	43
CO <sub>2</sub> Et	0.9	1.2	4.2	120
NO <sub>2</sub>	0.5	1.4	1.5	23.1
NH <sub>2</sub>	1.5	10.0	6.8	27.0
CH <sub>3</sub> O	0.09	0.5	0.5	2.2
FCH <sub>2</sub> O	0.7	1.6	1.5	3.4
F <sub>2</sub> CHO	0.9	1.2	1.8	9.9
F <sub>3</sub> CO	0.09	0.2	0.3	1.9

It was determined that methoxy and fluoromethoxyether substituted A-rings were the best alternatives to the 8248X A-ring. The synthetic scheme is outlined in Schemes 5 and 6.

### Scheme 5.

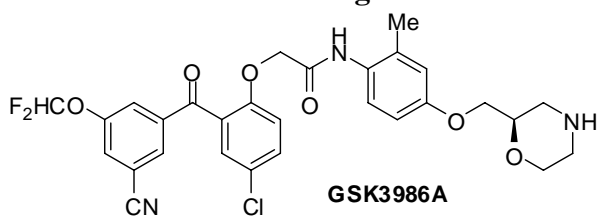


### Scheme 6.



Further C-ring SAR elaborations lead to **GSK3986A** which progressed to rat dose escalation studies (Figure 8).

**Figure 8.**



HIV-1 IC<sub>50</sub> = 0.3 nM  
K103N IC<sub>50</sub> = 0.3 nM  
Y181C IC<sub>50</sub> = 0.7 nM  
V106A IC<sub>50</sub> = 3.1 nM

Rat PK data  
CL = 5 mL/min/kg  
t<sub>1/2</sub> = 8.1 h  
AUC\* = 4.4 µg·h/mL  
%F = 28

Dog PK data  
CL = 17 mL/min/kg  
t<sub>1/2</sub> = 5 h  
AUC\* = 4.7 µg·h/mL  
%F = 87

hERG IC<sub>50</sub> = 29.8 µM  
solubility (FASSIF) = 0.082 mg/mL  
cLog P = 4.19

\* - 5 mpk PO in bioenhanced solution (DMSO/solutol/mannitol)

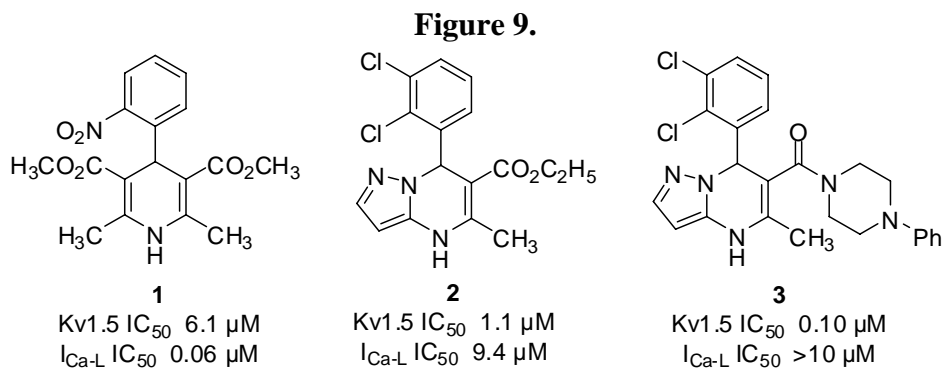
## “Discovery of pyrazolodihydropyrimidine Kv1.5 blockers”

*J. Lloyd, K. Atwal, W. Vaccaro, T. Huynh, H. J. Finlay, A. Kover, J. Prol, L. Yan, R. Bhandaru, C. Huang, M. L. Conder, T. Jenkins-west, H. Shi, L. Sun, H. Sun, D. Li, P. Levesque, Bristol-Myers Squibb Co., Princeton, NJ and Icagen Inc., Durham, NC*

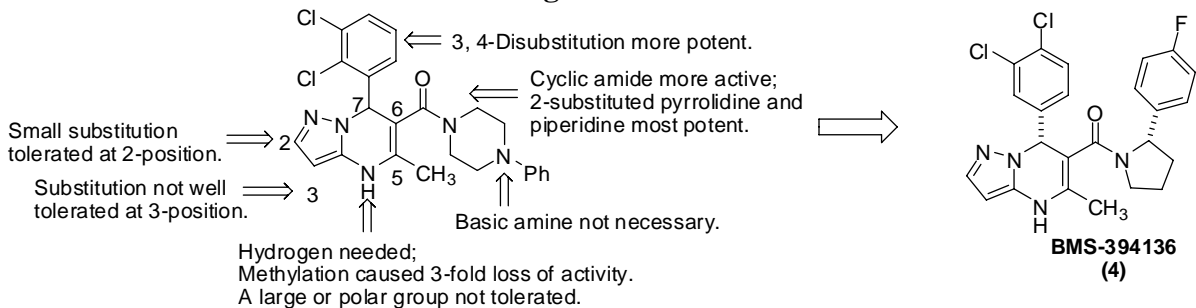
Atrial Fibrillation (AF) is a kind of arrhythmias in which the normal heart beat is disrupted by rapid and irregular electrical activity in the atria, causing the atria to be out of sync with the ventricles. Arrhythmias cause blood clot formation in the heart, and can lead to stroke or a blockage carried by the blood flow anywhere in the body's arteries. AF is the one of the most common cardiac arrhythmias in clinical practice, at present affects approximately 3 million in the US, and its prevalence is likely to increase with the aging of the populations.

Some currently available class III antiarrhythmic drugs can be used to treat AF. Their mechanism is to block the rapidly activating and deactivating  $K^+$  ( $I_{kr}$ ) current to prolong action potential duration (APD) and effective potential period (ERP). But inhibition of  $I_{kr}$  can cause prolonged QT syndrome, and prolongation of ventricular ERP predisposes to life threatening arrhythmia, which account of their serious side effects. In contrast, the ultra-rapidly activating delayed rectifiers  $K^+$  current ( $I_{kur}$ ) exists just in the human atrium and not the ventricles; and so blocking the according Kv1.5 channel offers a possible treatment of AF with an improved safety profile. In this poster the authors presented their effort to discover the clinical candidate of **BMS-394136** as an  $I_{kur}$  blocker.

It is known that the dihydropyridine calcium channel blocker nifedipine (**1**) is a nonselective Kv1.5 blocker (Figure 9). And The BMS discovery program began with a focused deck screening of calcium channel blockers. This effort resulted in the discovery a novel pyrazolodihydropyrimidine compound **2** with Kv1.5 inhibition activity. A simple amide derivatization of **2** could selectively remove calcium channel inhibition and it was anticipated that the pyrazolodihydropyrimidine was a good starting point for SAR studies.



The SAR effort focused on the pyrazolodihydropyrimidine core structure, resulting in the discovery of compound **4** (**BMS-394136**, Figure 10). This compound was selected as one of the pre-clinical candidates and eventually moved into clinical trial based on its good PK/PD profile at animal models. The related data are shown in Tables 4 and 5.

**Figure 10.****Table 4. PK/PD of BMS-394136.**

	Rat iv/po 10/20 $\mu\text{mol/Kg}$	Dog 10/5 $\mu\text{mol/Kg}$	Monkey 10/10 $\mu\text{mol/Kg}$
Clearance (mL/min/Kg)	18 $\pm$ 1.4	6.5 $\pm$ 2.5	27 $\pm$ 16
$V_{ss}$ (L/Kg)	1.65 $\pm$ 0.17	1.40 $\pm$ 0.15	7.9 $\pm$ 9.3
$t_{1/2}$ (h)	1.0 $\pm$ 0.09	9.4 $\pm$ 5.3	5.8 $\pm$ 1.9
MRT (h)	1.5 $\pm$ 0.05	3.99 $\pm$ 1.75	4.0 $\pm$ 2.1
$C_{max}$ ( $\mu\text{m}$ )	2.5 $\pm$ 0.8	0.80 $\pm$ 0.20	0.3 $\pm$ 0.2
$T_{max}$ (h)	0.28 $\pm$ 0.1	1.1 $\pm$ 0.40	2.3 $\pm$ 1.3
% F	35 $\pm$ 8	34 $\pm$ 5	25 $\pm$ 23

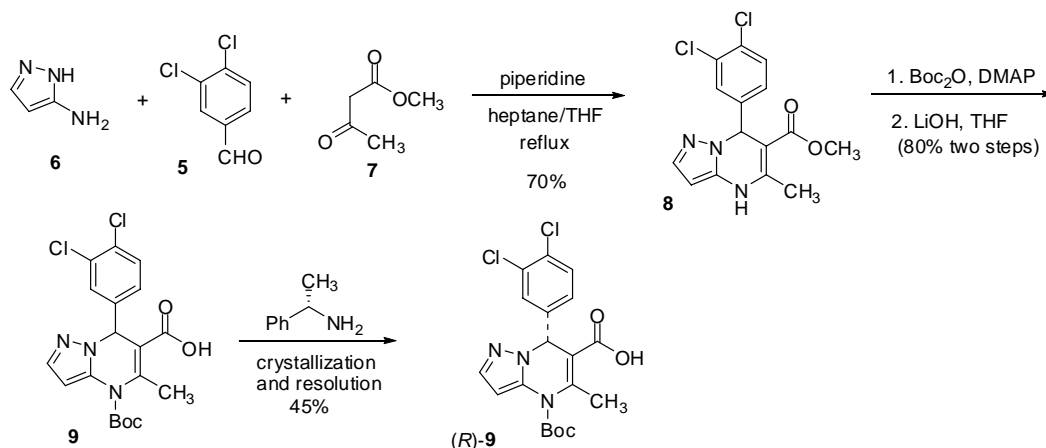
**Table 5. Selectivity of BMS-304136.**

	$IC_{50}$ ( $\mu\text{M}$ ) (% inh. at 10 $\mu\text{M}$ )
Kv1.5	0.053
$I_{kr}$	10.5
$I_{ks}$	>10 (37%)
$I_{Ca}$	>10 (7%)
$I_{Na}$	>10 (38%)
$I_{to}$	7.4
Kv1.1	0.06

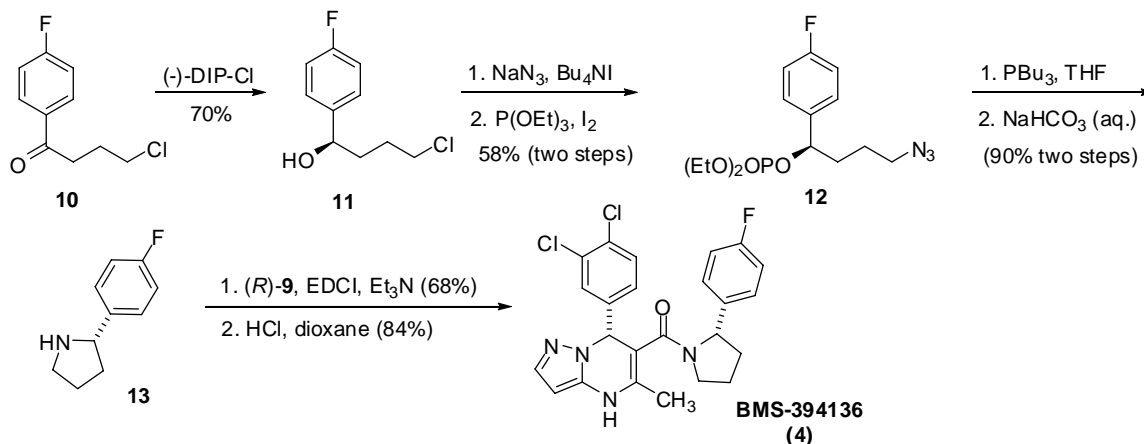
CYP inhibition (1A2, 2C9, 2C19, 2D6, 3A4) >6  $\mu\text{M}$

The chemistry to synthesize **BMS-394136** was shown in Schemes 7 and 8. The pyrazolodihydropyrimidine core was constructed in one step; and the desired enantiomer (*R*)-**9** was obtained by resolution. The chiral 2-aryl pyrrolidine **13** was prepared from chloro ketone **10** in 5 steps, and the chiral center was introduced by chiral reduction of the ketone. The final product **4** was obtained by coupling the two intermediates followed by de-protection.

### Scheme 7.



### Scheme 8.

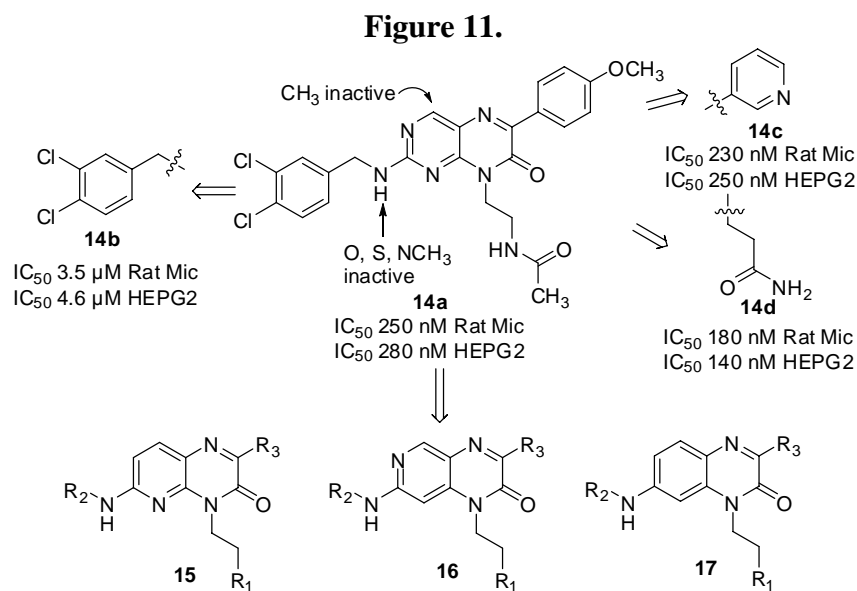


## “Potent, selective, and metabolically stable stearyl-CoA desaturase (SCD) inhibitors for the treatment of obesity and diabetes”

Dmitry O. Koltun, et al., CV Therapeutics Inc., CA, USA; ASINEX Ltd. Moscow, Russia and Pharmacopeia Drug Discovery, Inc., NJ, USA

The synthesis of monounsaturated fatty acids is a critical step in the formation of triglycerides and the overall process of energy storage. Inhibition of the synthesis of monounsaturated fatty acids may lead to a decrease in lipid storage in liver and adipose tissue, and an increase in energy expenditure thus leading to weight loss and increase in insulin sensitivity. Stearyl CoA desaturase (SCD) is responsible for converting long-chain saturated fatty acids (e.g. stearic) into 9-cis-unsaturated fatty acids (e.g. oleic). The SCD gene is most highly expressed in liver and adipose tissue; and it is a highly regulated gene, up-regulated during food consumption and hyperinsulinemia, and down-regulated during fasting. The reduction in SCD activity could dramatically reduce adiposity and restore the normal phenotype in *ob/ob* and dietary induced obesity mice models, which verified the therapeutic potentials of inhibition of SCD.

The authors of this poster showcased how they pursued novel IP position in this field. First they carried out an independent screen of ~5.2 million compounds, and the pteridione hit such as **14a** was found to have IP space for further development (Figure 11).



The first round SAR studies focused on the pteridione was not successful, over 250 compounds synthesized, with no significant improvement over the initial hit **14a**. But the bicyclic core was the major difference from the competitors' compounds, and so the second round search was focused on the modification of the fused core structure. Several new scaffolds were produced by variation of the number or position of heteroatom on the core structure. Some new scaffolds were depicted in Figure 11. Among these new scaffolds, the quinoxalinone scaffold in generally had better potency, and several compounds had sub-nanomolar activity in microsomal assay, with around 500 fold improvement in potency over the initial hit **14a**. Some selected data are listed in Table 6.

**Table 6. Optimization of potency in modified scaffold 17.**

Compd.	R <sub>1</sub>	R <sub>2</sub>	R <sub>3</sub>	IC <sub>50</sub> (nM)	
				Rat Microsomal	HepG2
<b>17a</b>	NHCOMe	3,4-dichlorobenzyl	4-methoxyphenyl	110	8.6
<b>17b</b>	NHCOMe	3-(trifluoromethyl)benzyl	4-methoxyphenyl	93	3.3
<b>17c</b>	NHCOMe	3-(trifluoromethyl)benzyl	3-pyridyl	140	13
<b>17d</b>	NHCOMe	3-(trifluoromethyl)benzyl	4-ethylphenyl	42	2.9
<b>17e</b>	NHCOMe	3-methylbenzyl	4-methoxyphenyl	18	--
<b>17f</b>	NHCOMe	3,4-dimethylbenzyl	4-methoxyphenyl	26	--
<b>17g</b>	NHCOMe	4-chlorobenzyl	4-methoxyphenyl	4.3	--
<b>17h</b>	NHCOMe	4-chloro-3-(trifluoromethyl)benzyl	4-methoxyphenyl	0.6	0.1
<b>17i</b>	NHCOMe	4-fluoro-3-methylbenzyl	4-methoxyphenyl	0.5	3
<b>17j</b>	NHCOMe	(4-trifluoromethyl-2-pyridyl)methyl	4-methoxyphenyl	39	--

All analogues from the new scaffolds that were selected for follow-up testing showed greater than 100-fold selectivity for  $\Delta 9$ -desaturase over  $\Delta 5$  and  $\Delta 6$ , and greater than 50% stability in HLM and RLM (30 min. incubation).

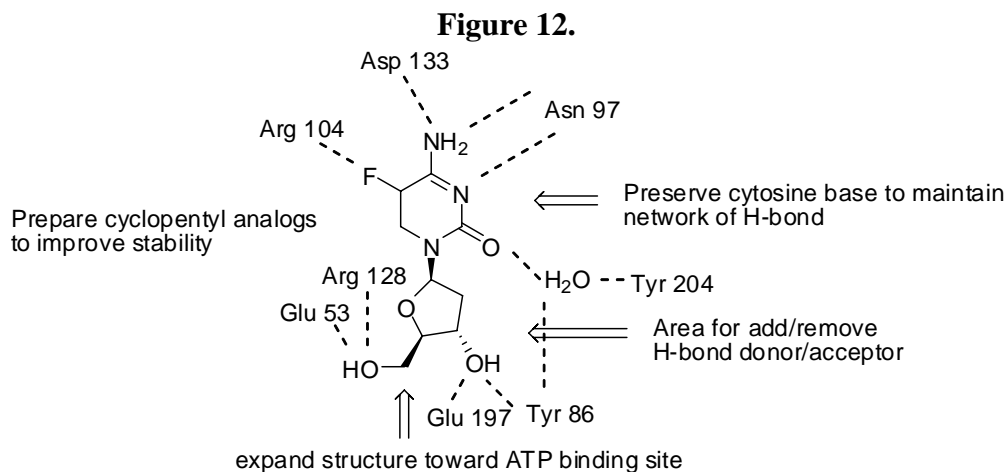
---

### “Lead Optimization and Structure-Based Design of Deoxycytidine Kinase Inhibitors with Potent In Vitro and In Vivo Activity”

Theodore C. Jessop, et al., Lexicon Pharmaceuticals, Inc., Princeton, NJ, Lexicon Pharmaceuticals, Inc., Corporate Headquarters, The Woodlands, TX, Trius Therapeutics, Inc, San Diego, CA and ActiveSight, San Diego, CA

Deoxycytidine kinase (dCK) is a nuclear enzyme with particularly high expression in lymphocytes; it is involved in the nucleoside salvage pathway by catalyzing the phosphorylation of pyrimidine and purine deoxynucleosides. Lexicon has investigated the physiological and behavioral functions for many human genes by studying the corresponding mouse genes in KO animals. The phenotype observed in deoxycytidine kinase KO mice identified dCK as a potential drug target in multiple disease states within cancer. This poster illustrated the discovery of **LP-661438**, a potent and selective inhibitor of dCK, capable of blocking the uptake (salvage) of deoxycytidine by T lymphocytes *in vitro* and *in vivo*; and demonstrated the power of structure-based drug design.

The work began with the investigation of the co-crystal structures of 5-fluorodeoxycytidine (5-FdC) in the substrate binding pocket of dCK, which revealed an array of interactions (Figure 12). Phe 96 and Phe 157 provide a hydrophobic environment above and below the cytosine base to help constrain the substrate in the binding pocket. There also existed a net work of hydrogen bond interactions as depicted. Based on this observation, new compounds were designed. In these new compounds, the cytosine base in 5-FdC was kept intact to maintain network of hydrogen bond, while the deoxyribose was changed to cyclopentyl group to improve stability and also offer new site for further derivatization.



Among those cyclopentyl analogues, allylic alcohol **18** was identified as an early lead. In the process of making **18**, ester **19** was discovered to be more potent and thereafter served as the lead for further development. After the initial SAR effort, two scaffolds **20** and **21** with nM activities were discovered (Figure 13), and some of the data for these two scaffolds are listed in Table 7. In general, the compounds with an amide linkage displayed improved potency and a reduced disparity between the primary and cell based assay.

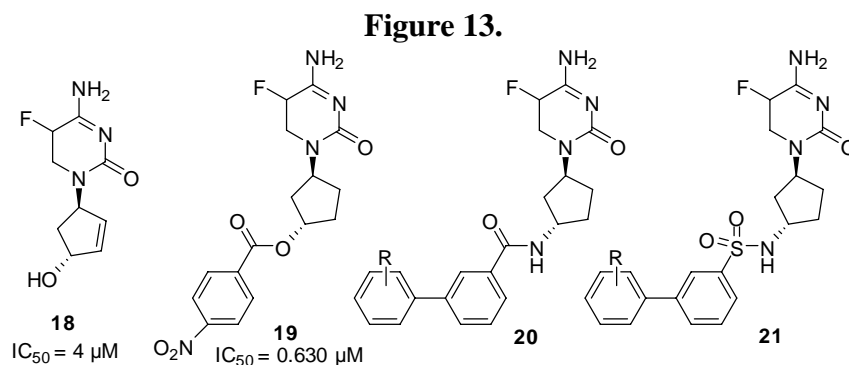


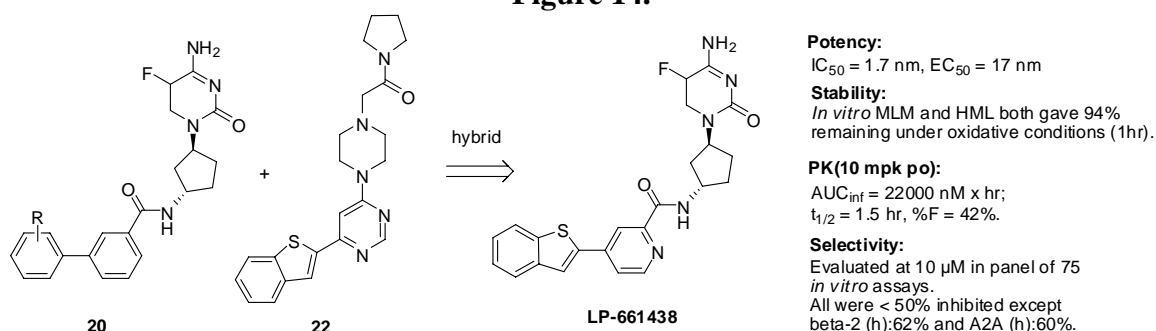
**Table 7. Data for selected biphenyl amides and biphenyl sulfonamides.**

Compound	R	$IC_{50}$ ( $\mu M$ )	$EC_{50}$ ( $\mu M$ )	$AUC_{inf}$ (nM hr)	$C_{max}$ (nM)	$t_{1/2}$ (hr)	$t_{max}$ (hr)	CL (mL/min/Kg)	$V_z$ (L/Kg)	% F
<b>20a</b>	H	0.26	0.91							
<b>21a</b>	H	0.12	0.6							
<b>20b</b>	4-methoxy	0.03	0.1	3800	3400	1.6	0.3	18	1.3	17
<b>21b</b>	4-methoxy	0.064	0.31	600	300	1.2	0.8	63	4.4	9
<b>20c</b>	4-trifluoromethyl	0.049	0.23							
<b>21c</b>	4-trifluoromethyl	0.1	0.29							
<b>20d</b>	4-chloro	0.042	0.27	15800	16200	0.8	0.3	3	0.2	12
<b>21d</b>	4-chloro	0.051	0.24	5200	1000	2.1	2	140	16	nd
<b>20e</b>	4-chloro-2-methyl	0.021	0.17	10800	10100	1.3	0.3	20	1.6	58
<b>21e</b>	4-chloro-2-methyl	0.021	0.29	2300	1500	1.6	0.3	23	3	15

A different type lead represented by compound **22** was discovered by high throughput screening. In the co-crystal with dCK, compound **22** is bound in the active site of dCK different from 5-FdC. The top part picked up much less hydrogen bond interactions in the cytidine base binding pocket, but the bottom aromatic part opened a new hydrophobic pocket by the rearrangement of four amino acid residues. Docking of the amide scaffold **20** into the new binding pocket previously occupied by **22** shown that the biphenyl part of scaffold **20** could be placed in this newly formed pocket in a similar way. These observations allowed the design of a hybrid molecule that combined the cytidine base from **20** with the bottom parts from the new scaffold. These new hybrid molecules could pick up both the dense network of hydrogen bond contacts and the hydrophobic interactions (Figure 14). One of the hybrid molecules, compound **23** (**LP-661438**) was

selected for further development, it was a potent, selective dCK inhibitor and capable of blocking the salvage of deoxycytidine by T lymphocytes *in vitro* and *in vivo*.

**Figure 14.**

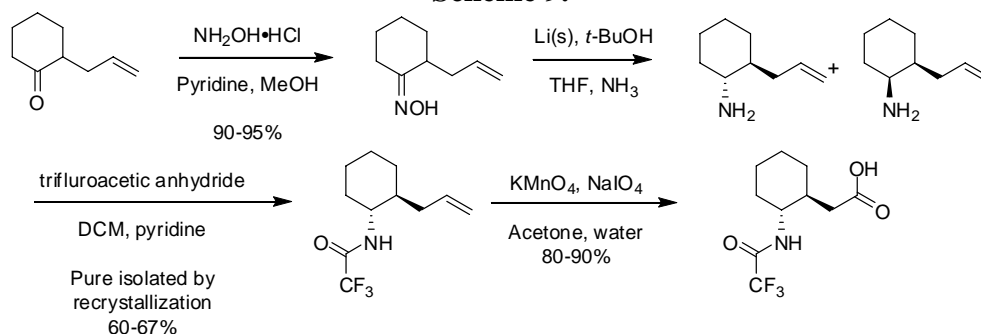


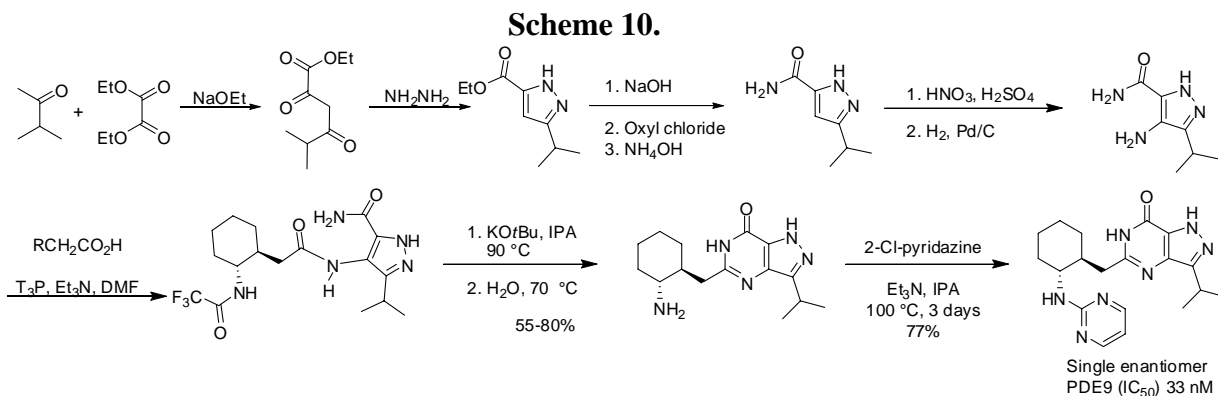
### Synthesis of *N*-projected *trans*-2-aminocyclohexyl acetic acid for the preparation of potent and selective PDE-9 inhibitors

John B. Etienne, Michael DeNinno, Cynthia Eller-Zarbo, E. Michel Gibbs, William J. Zavadiski, Paul E. Genereux and Li J. Yu, Pfizer Global Research & Development, Groton laboratories, Pfizer Inc, Groton, CT

About 15 million Americans have diabetes with about 5 million of these having undiagnosed type-2 diabetes. Cyclic GMP phosphodiesterases (PDE) 5 and 9 both expressed in human skeletal muscle are potential therapeutic target for the treatment of type-2 diabetes. Recent clinical data provide strong rationale for the use of CGMP PDE inhibitors in the treatment of type-2 diabetics. Reduced glucose, triglyceride and insulin levels have been observed in PDE 9 knock out mice upon treatment with a PDE 9 inhibitor. The synthesis of a Pfizer compound is shown in Schemes 9 and 10.

**Scheme 9.**





### Synthesis and Biological Activity of *N*<sup>4</sup>-aryl-6-arylmethyl-7*H*-pyrrolo[2,3-*d*]pyrimidine-4-amines as Multiple Receptor Tyrosine Kinase Inhibitors and Antiangiogenic Agents

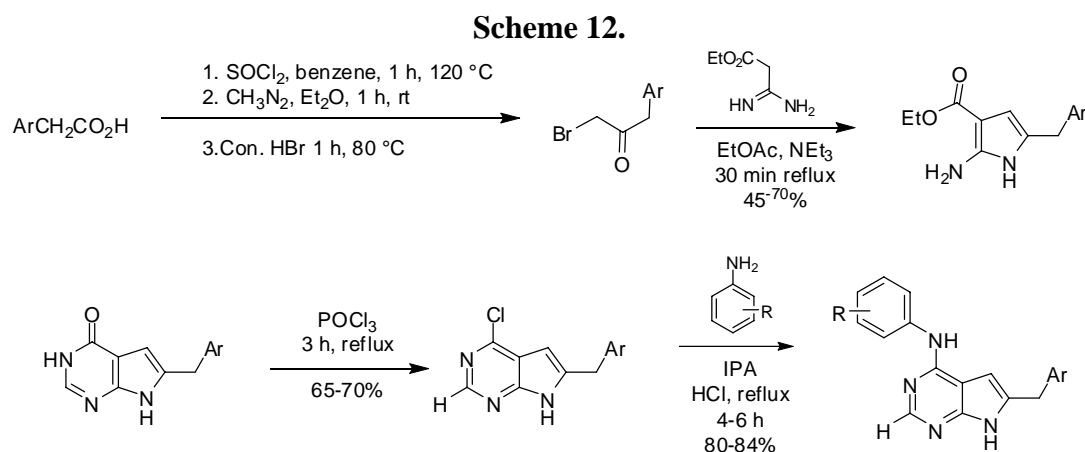
Sonali Kurup, Aleem Ganglee, Michael A Ihnat and Dixy Green, Division of Medicinal chemistry, Duquesne University, Pittsburg, PA and Department of cell biology, University of Oklahoma, Oklahoma City, OK

Receptor tyrosine kinases (RTKs) have important functions in signal transduction pathways that regulate cell proliferation, differentiation and growth under normal cell function as well as under disordered conditions. Dysfunctional, hyperactive growth factor RTKs including PDGFR, FGFR, VEGFR, IGF1R and EGFR among others have been associated with several cancers where they play a pivotal role in tumor angiogenesis.

Angiogenesis is the formation of new blood vessels from existing vasculature and occurs in normal adults during wound healing, pregnancy and corpus luteum formation. It requires the transduction of signals from the extracellular domain of endothelial cells to the nucleus which is mediated by RTKs. Angiogenesis is also associated with diabetic retinopathies, psoriasis and cancer. Solid tumors require angiogenesis to grow beyond 1-2 mm in size. Also, metastasis requires the presence of blood vessels to allow entrance into circulation to form tumors at sites distal to the primary tumor. Inhibition of tumor angiogenesis prevents the growth and metastasis of several types of solid tumors. Thus, inhibition of angiogenesis via RTK inhibition provides an attractive target for the treatment of cancer. Single RTK inhibition by small molecules such as erlotinib and gefitinib has been well established as a possible mechanism of cancer therapy. However, in several tumors, multiple RTKs are simultaneously overexpressed and have been suggested to act individually or in concert during angiogenesis. Second generation RTK inhibitors include single agents that target multiple RTKs. Both sorafenib, an inhibitor of VEGFR, PDGFR and Raf-1 and sunitinib, an inhibitor of VEGFR-1, VEGFR-2, Flt-3, PDGFR, c-kit and CSF-1 have been approved for renal cell carcinoma. Simultaneous inhibition of multiple RTKs provides synergistic or additive effects and reduce resistance and toxicity. Single agents with multiple RTK inhibitory activity thus represent a useful approach for cancer therapy.

Gangjee, *et al.* previously reported a series of  $N^4$ -aryl-6-arylmethyl-7*H*-pyrrolo[2,3-*d*]pyrimidine-2,4-diamines as multiple RTK inhibitors. A 2-amino moiety was incorporated as an important integral part of the design of these pyrrolo[2,3-*d*]pyrimidines to provide an additional hydrogen bond with the Hinge region of the ATP binding site of RTKs, compared to similar RTK inhibitors without the 2-amino moiety. The flexible 6-benzyl substitution was incorporated to allow for multiple conformations of the side chain and thereby afford multiple binding modes.

Gangjee, *et al.* demonstrated that variation of the phenyl substitutions in the 6-benzyl moiety and the 4-anilino moiety determined both the potency and specificity of inhibitory activity against various RTKs. In order to demonstrate that the 2-amino moiety does indeed afford an increase in potency, owing to an additional hydrogen bond with the Hinge region, 2-*des* NH<sub>2</sub> analogs also were synthesized (Scheme 12). RTK inhibitory activities of the compounds were evaluated using human tumor cells known to express high levels of EGFR, VEGFR-2, VEGFR-1 and PDGFR- $\beta$ . Whole cell assays were used for RTK inhibitory activity since these assays afford more meaningful results for translation to *in vivo* studies. The effect of compounds on cell proliferation was measured using A431 cancer cells, known to overexpress EGFR. The antiangiogenic effect of the compounds was evaluated using the chicken embryo chorioallantoic membrane (CAM) assay, a standard test for angiogenesis. Since the IC<sub>50</sub> values of compounds vary under different biological conditions, a standard compound in each of the evaluations was used. PD153035 was used as a standard for EGFR inhibition. AG1295 was used for PDGFR- $\beta$ . SU5416 was used for VEGFR-2 and in the CAM assay, and CB676475 was used for VEGFR-1 inhibition. Cisplatin was used as a standard in A431 cytotoxicity assay.

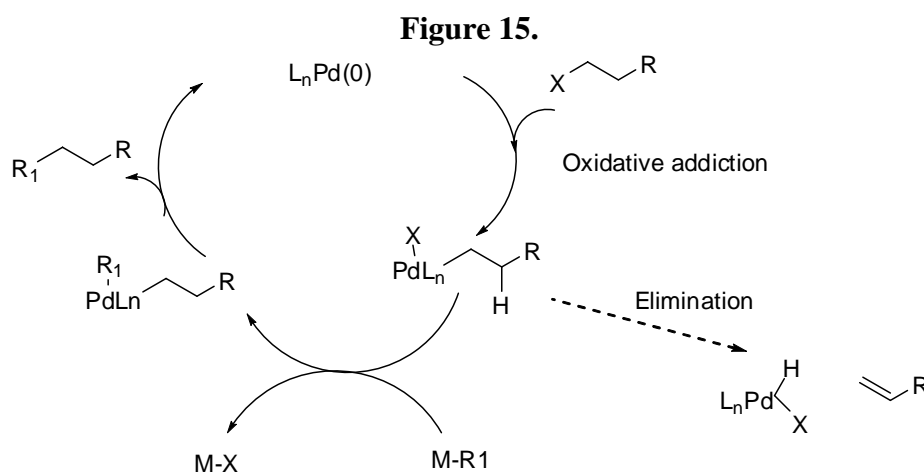


VEGFR-1 inhibition did not improve for the 2-*des* amino analogs compared to the 2-amino substituted compounds respectively and also compared to the standard CB676475. The 2-amino substituted compounds showed moderate PDGFR- $\beta$  inhibition being approximately 2-fold and 4-fold less potent than the standard AG1295. The PDGFR- $\beta$  inhibition decreased for the corresponding 2-*des* amino analogs. The PDGFR- $\beta$  inhibition did not improve for the 2-*des* amino analogs compared to the 2-amino substituted compounds. All of the compounds showed poor antiangiogenic activity compared to the

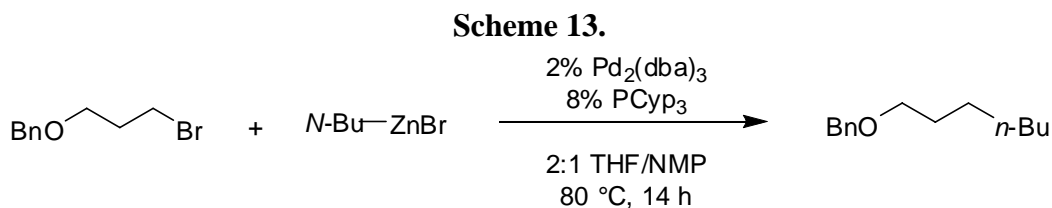
standard SU5416, however the 2-*des* amino analogs showed a decrease in the antiangiogenic.

## Transition Metal Mediated Reactions

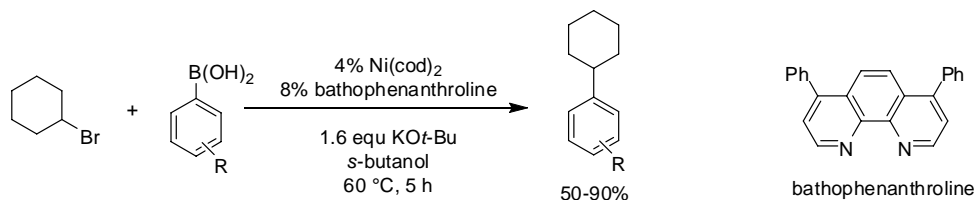
Palladium and Nickel catalyzed cross-coupling reactions are the most useful methods for generating carbon bonds (Figure 15). Unfortunately, all investigations have focused on reactions of aryl or alkenyl electrophiles. Reports of coupling of alkyl electrophiles are relatively rare except for activated compounds that lack  $\beta$ -hydrogens. It is believed that coupling of simple halides or sulfonates is preceded by slow oxidative addition followed by rapid elimination.



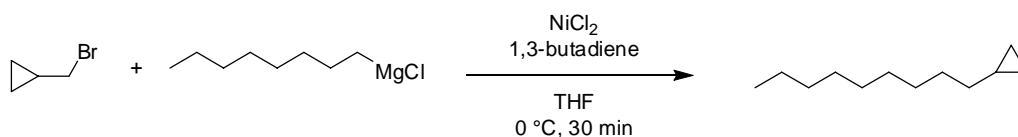
Fu and Zhou from MIT reported a single method which achieves the cross coupling of a range of  $\beta$ -hydrogen containing primary alkyl iodide, bromide, chloride, and tosylates with a series of alkyl-, alkenyl-, and arylzinc halides (*J.Am.Chem. Soc.* **2003**, *125*, 12527). This process is compatible with a variety of functional group including esters, amides, imides, nitriles and heterocycles. They determined that Pd/PR<sub>3</sub> systems like PCy<sub>3</sub> or P(*t*-Bu)<sub>2</sub>Me can serve as effective catalysts for the Suzuki coupling reaction of primary alkyl bromide, chloride and tosylates with trialkylboranes (Scheme 13).



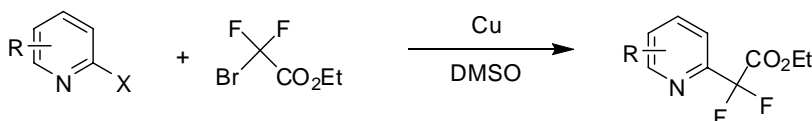
They also developed a catalyst system that achieves the Suzuki coupling reaction of inactivated secondary alkyl bromides and iodides (Scheme 14). The ability to couple readily available easy-to-handle boronic acid is an attractive feature of this process (*J.Am.Chem. Soc.* **2004**, *126*, 1340; *J. Org. Chem.* **1998**, *63*, 461).

**Scheme 14.**

Kambe's group reported a novel method for the cross-coupling reaction of Grignard reagents with alkyl chlorides, bromides, and tosylates with the aid of a Ni catalyst (Scheme 15). This reaction proceeds with the use of primary and secondary alkyl or aryl magnesium halides under mild conditions. The use of 1,2 butadiene as an additive instead of phosphine ligands is the key and interesting factor which gives high yields of cross-coupling products (*J. Am. Chem. Soc.* **2002**, *124*, 4222).

**Scheme 15.**

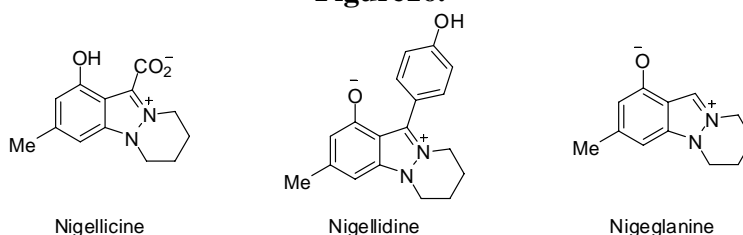
In the process of drug design the incorporation of fluorine substituents is a powerful and widely employed tactic to circumvent metabolism issues arising from in vivo C-H bond oxidation (Scheme 16). Copper-mediated cross-coupling of 2-halopyridines with ethyl bromodifluoroacetate were demonstrated by Michel Ashwood's group from Merck. Kobayashi had reported similar reactions of 2-bromopyridine with methyl iododifluoroacetate. But the starting ester is very expensive and unavailable in bulk quantities. Ethyl bromodifluoroacetate solved these issues. The reaction has done at 50 °C in DMSO for 2 hours (*Tetrahedron Lett.* **2002**, *43*, 9271; *J. Am. Chem. Soc.* **2005**, *127*, 8826).

**Scheme 16**

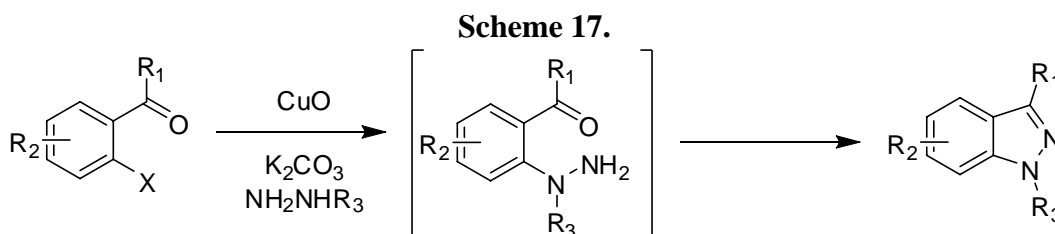

---

### “Synthesis of Indazoles Electrophilic Amination Approaches”

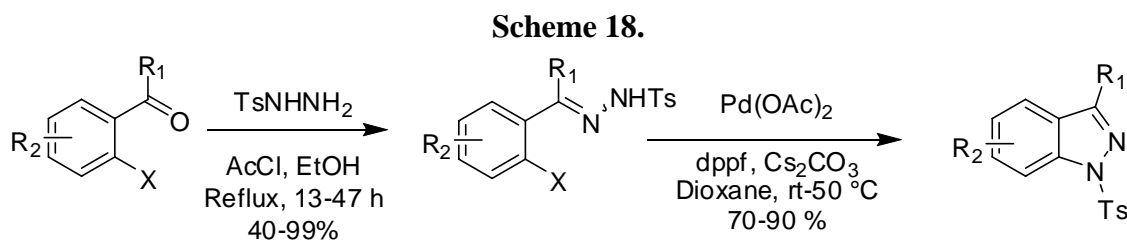
Indazoles have very important biomedical application in anti-inflammatory, antitumor, anti-HIV, antidepressant and contraceptive therapeutic areas. The indazole nucleus is rarely encountered in nature. Only three natural products nigellicine, nigellidine, nigeplanine have appeared in the literature and two of them are 3-substituted indazoles.

**Figure 16.**

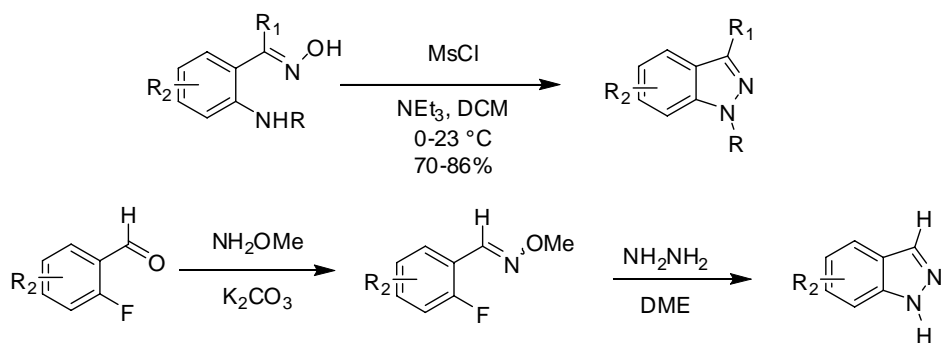
There are several methods available for the synthesis of substituted indazoles. Unfortunately, most of them involve a number of tedious steps, high temperature, poor substrate scope and expensive catalysts. The following are some interesting approaches towards the synthesis of Indazoles via electrophilic amination. Olmo's group report a general method for the one-step regioselective synthesis of 1-alkyl/aryl-1*H*-indazoles from ortho-halogenated alkanoylphenones, benzophenones, and arylcarboxylic acid via copper-catalyzed amination followed by intramolecular dehydration (Scheme 17). They used 0.2% CuO in the presence of K<sub>2</sub>CO<sub>3</sub> as a catalyst (*Org. Lett.* **2007**, 9,525; *J. Biol. Chem.* **2004**, 279, 49617).



Different functionalized alkyl ketones, diaryl ketones, and benzoic acid derivatives were efficiently coupled with several hydrazines. It was found that ligands commonly used as catalyst for amination were ineffective for this cyclization. Inamoto, *et. al* reported the synthesis of 3- substituted indazoles and benzoisoxazoles using an intermolecular Pd-catalyzed amination reaction of hydrazones under mild conditions (Scheme 18, *Tetrahedron Lett.* **2007**, 63, 2695).



Stambuli's group achieved the synthesis of 1*H*-indazoles from *O*-aminobenzoximes by the activation of the oxime in the presence of the amino group (Scheme 19). The reaction occurred with a variety of substituted *O*-aminobenzoximes using methanesulfonic chloride and triethyl amine. The advantage of this reaction is milder conditions, better yield and scalability (*Org. Lett.* **2008**, 10, 1021; *J. Org. Chem.* **2006**, 71, 8166).

**Scheme 19.**

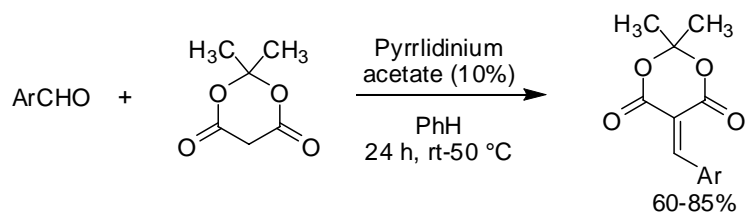

---

**“Meldrum’s acid derivative as powerful and versatile electrophiles in carbon-carbon bond forming reactions”**

*A.M. Dumas, E. Fillions*

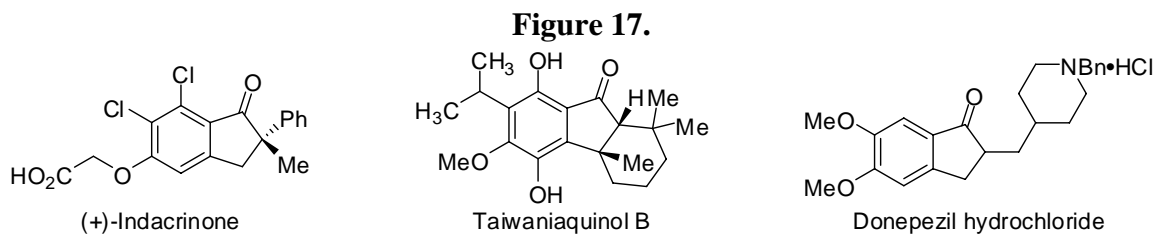
Alkylidene Meldrum’s acid are highly reactive 1,1-deactivated alkenes that have been used extensively as acceptors in 1,4-addition of a variety of organometallic reagents, as dienophile and diene in Diels-Alder and hetero Diels-Alder reactions respectively. Although many methods have been reported for the Knoevenagel condensation of aldehydes and Meldrums acid, most are not simple and general or use unconventional conditions and hazardous reagents. Fillion *et. al* reported that alkylidene Meldrum’s acids form readily under mild conditions and this reaction is general highly functional group compatible and can be scaled-up easily.

In early 1961, Snyder noted that the condensation of an aldehyde and Meldrum’s acid can be complicated by competing Michael addition of alkylidene Meldrums’s acid. This was avoided by performing the reaction in dilute organic solvent such as benzene. Catalytic amount of pyrrolidinium acetate was added to the reaction mixture to facilitate the condensation and reverse reaction of unwanted Michel adduct to product (Scheme 20).

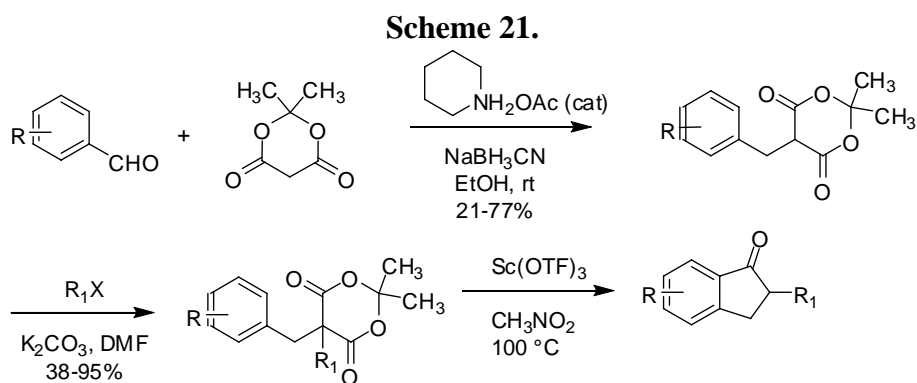
**Scheme 20.**

Fillion *et. al* also reported intermolecular Friedel-Crafts acylation of aromatic Meldrum’s acid derivatives catalyzed by metal trifluoromethanesulfonate. The intermolecular Friedel-Crafts acylation is the most powerful tool for carbon-carbon bond formation in the field of synthetic organic chemistry. Indanones, tetralones, benzosuberones and related compounds are synthesized by this method and these structural moieties have proven synthetic utility in numerous biologically active natural products and play a major role in medicinal chemistry and the development of pharmaceuticals. The antihypertensive drug

indacrinone, taiwaniaquinol B and the acetylcholinesterase inhibitor donepezil hydrochloride all contain a 1-indanone core (Figure 17).

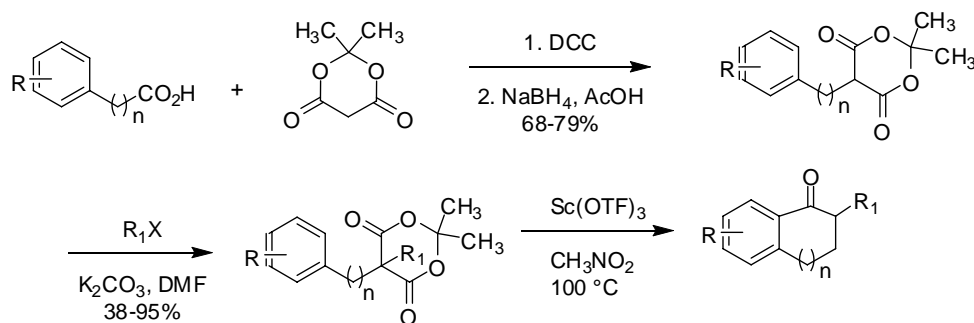


Benzylmeldrum's acids were successfully prepared from substituted benzaldehyde and Meldrum's acid with  $\text{NaBH}_4\text{CN}$  at room temperature in the presence of a catalytic amount of piperidinium acetate in EtOH (Scheme 21). Substrates of longer length were synthesized by using Tsukamoto's mythology. Carboxylic acids were coupled to Meldrum's acid with use of DCC to form the isopropylidene acylmalonates that were subsequently reduced with  $\text{NaBH}_4$  in AcOH to the corresponding 5-alkyl Meldrum's acids. Symmetrical 5,5-dibenzyl substrates were prepared in one step by reacting Meldrums acid with 2 equivalents of appropriate benzyl bromide in DMF using  $\text{K}_2\text{CO}_3$  as base.



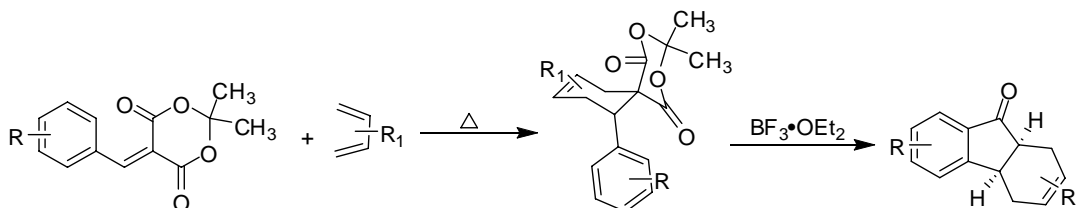
The scope of intramolecular Friedel-Crafts acylation of 5- benzyl meldrum's acids has been defined by varying substitution and electron pattern ability of pi-nucleophile unit, as well as substitution at the beta-position to generate a diversity of functionalized 1-indanones in yields ranging from 13% to 86% (Scheme 22). It was found that the Lewis acid  $\text{Sc}(\text{OTf})_3$ , effectively catalyzes the reaction. 1-tetralones were readily formed with higher yields in preference to 1-indanones and 1-benzosuberones under mild conditions.

### Scheme 22.



Fillion also reported the one-pot synthesis of tetrahydrofluorenones, the core 6-5-6-tricyclic structural motif found in norditerpenoid natural products, taiwaniaquinol B, from alkylidene Meldrum's acid via thermal Diels-Alder/BF<sub>3</sub>·OEt<sub>2</sub>-catalyzed Friedel-Craft acylation reaction (Scheme 23).

### Scheme 23.



For current references on this work, see *J. Org. Chem.* **2006**, *71*, 409; *J. Org. Chem.* **2008**, *73*, 2920; *J. Org. Chem.* **2006**, *71*, 9899; *J. Org. Chem.* **2008**, *73*, 2738; *J. Org. Chem.* **2005**, *70*, 1316.

---

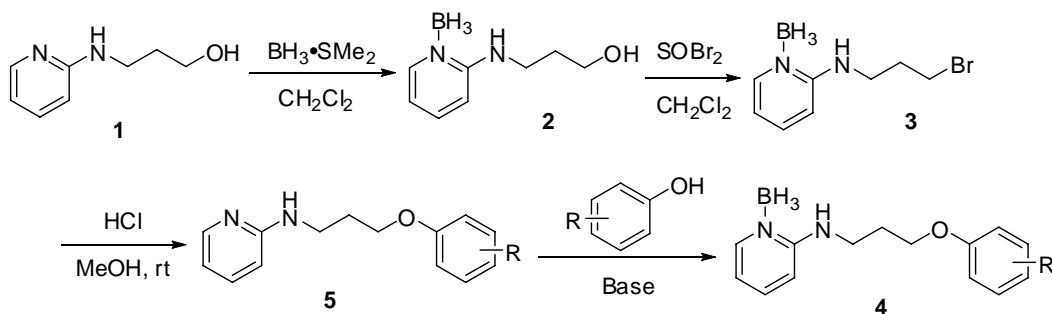
### “Novel Use of Borane as an Easily Removable Protecting Group for Pyridine”

Matthew Zajac, GlaxoSmithKline, King of Prussia, PA

This poster detailed efforts toward the development of novel protecting strategies for pyridine moieties. Pyridine functionality is a common core component in many pharmaceutically interesting compounds. Unfortunately, the presence of a pyridine nitrogen can often cause synthetic problems in the presence of electrophiles (*i.e.*, alkylations or acylations). Currently, few practical protecting strategies exist for pyridines, and synthetic routes must be planned around the installation of the pyridine unit.

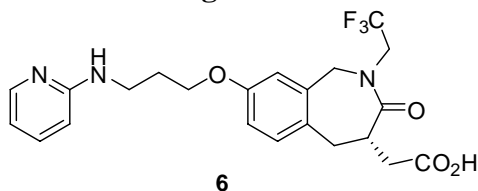
Typical protecting strategies for pyridine nitrogens generally center around the formation of the N-oxide, however this process is often impractical for scale-up, and removal can be problematic. The process group at GSK has developed an alternate strategy for protecting pyridyl nitrogens using borane as outlined in Scheme 24. These pyridyl-borane complexes can be handled easily and purified using silica gel chromatography. Removal is also straight forward using hydrogen chloride (similar to the removal of a Boc group).

**Scheme 24.**



This protecting strategy was successfully employed on multi-kilogram scales during the synthesis of a vitronectine inhibitor **6** (Figure 18).

**Figure 18.**



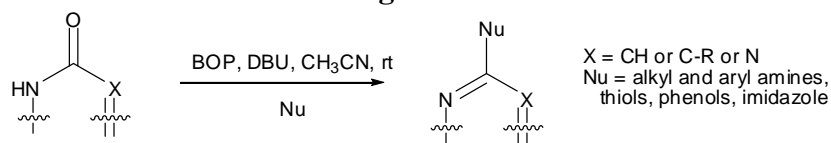
---

### “Serendipitous Synthetic Discoveries: A tale of Phosphonium and Oxybenzotriazole Chemistry”

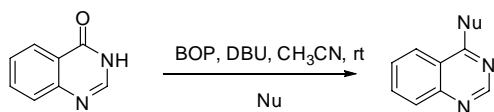
*Zhao-Kui Wan, Wyeth*

This presentation detailed efforts toward the development of a general synthetic methodology for the direct amination of cyclic amides and ureas. This methodology provides an easy route for the diversification of biologically preferred cores found in many natural products and kinase inhibitors (Figure 19).

**Figure 19.**

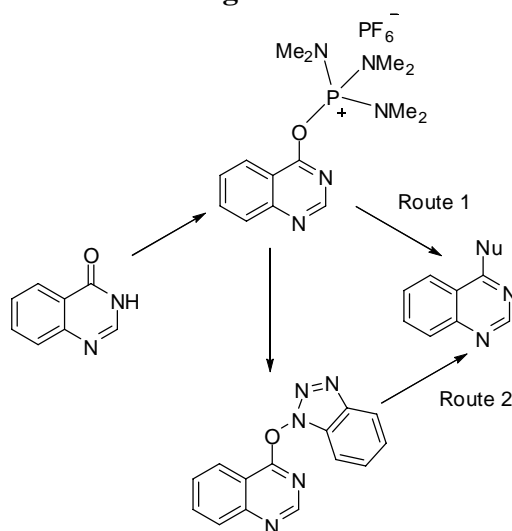


Initial method development utilized 4-hydroxyquinazolines and a variety of nucleophiles including amines, phenols, and thiols. These studies concluded that, in the presence of BOP and the organic base DBU, excellent conversion could be achieved under mild conditions (Table 8).

**Table 8.**

Entry	Nucleophile	Yield	Entry	Nucleophile	Yield
1	$t\text{-BuNH}_2$	64%	5		92%
2		88%	6		93%
3	$\text{H}_2\text{N}-\text{CH}_2-\text{CO}_2\text{Me}$	84%	7		84%
4		78%			

The mechanism of the nucleophilic addition may be occurring via two separate reaction pathways depending on the relative strength of the nucleophile as compared to HOBT (Figure 20).

**Figure 20.**

This general methodology represents an attractive route to a wide range of biologically relevant cores and preferred structures using mild conditions.

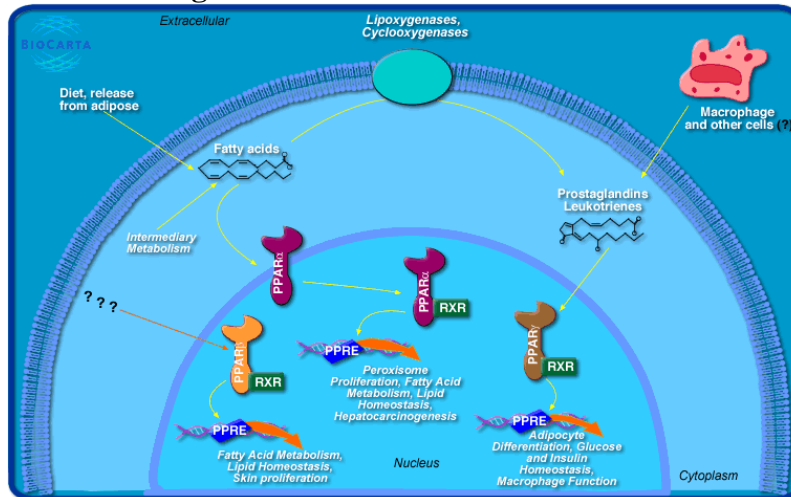
---

**“Synthesis and Biological Evaluation of Azole Acid Analogs as Novel, potent Dual alpha/gamma Activators”**

*Zhang Hao, Bristol-Myers Squibb Co.*

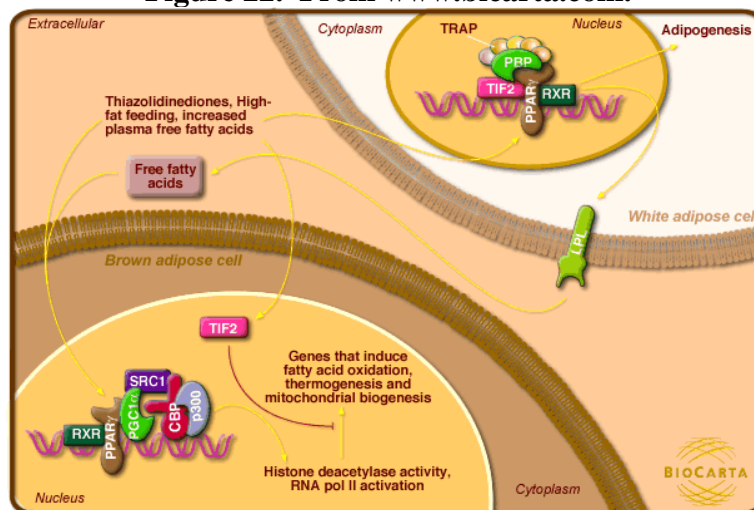
This presentation details continuing efforts to identify novel potent and efficacious PPAR $\alpha$ / $\gamma$  dual activators. Similar to other nuclear hormone receptors, PPAR acts as a ligand activated transcription factor (Figure 21).

**Figure 21. From www.bicarta.com.**



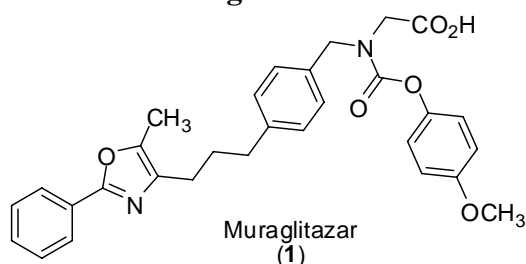
Upon binding fatty acids or hypolipidemic drugs, PPAR $\alpha$  interacts with RXR and regulates the expression of target genes. These genes are involved in the catabolism of fatty acids. Conversely, PPAR $\gamma$  is activated by prostaglandins, leukotrienes, and anti-diabetic thiazolidinediones and affects the expression of genes involved in the storage of the fatty acids (Figure 22). Both receptors play an important role in insulin sensitivity and adipogenesis. Like PPAR $\alpha$  and other members of this gene family, PPAR $\gamma$  activates transcription in concert with a number of coactivators including Src-1 and Tif2, and the full cascade of activation is complex and not yet fully understood. Given the importance of these pathways in the regulation of insulin and free fatty acid levels, the PPAR family of receptors has become a focal point in the area of type II diabetes research.

**Figure 22. From www.bicarta.com.**



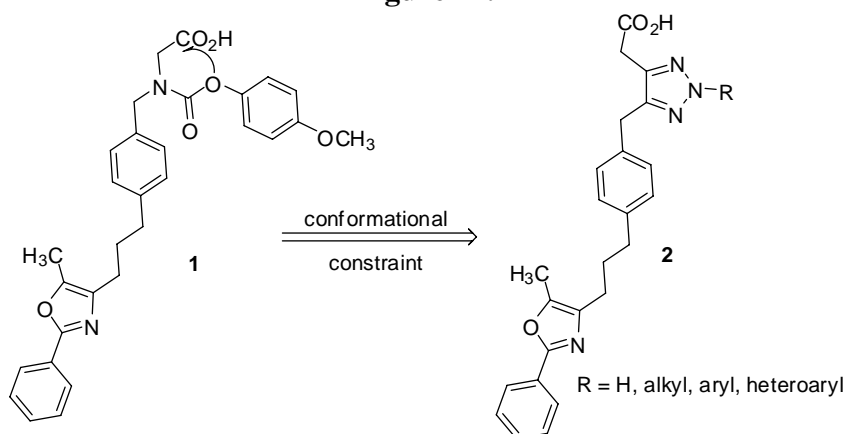
Previously, Muraglitazar (**1**, Figure 23) had been identified as non-thiazolidinedione PPAR $\alpha/\gamma$  dual agonist with potent activity in vitro ( $EC_{50}$  = 320 nM in alpha and 110 nM in gamma). When in vivo studies were carried out on genetically obese mice at 10 mg/kg/d reduced levels of plasma triglycerides were observed (-33%).

**Figure 23.**



In an effort to further reduce triglyceride plasma levels, modification of **1** was undertaken. Efforts to induce more conformational rigidity in the acid moiety was initially attempted with the rationale that such structures might more closely mimic thiazolidinediones. This led to the development of a series of triazoles of which significant conformational constraint is incorporated near the acid portion of the molecule (Figure 24).

**Figure 24.**



Incorporation of this new series in vivo showed further reductions in the level of plasma triglycerides. In particular one compound (R = Ph) showed reductions of greater than 50% at 10mg/kg/d. This series displays an excellent ADME profile and continues to be evaluated as a preclinical candidate.

---

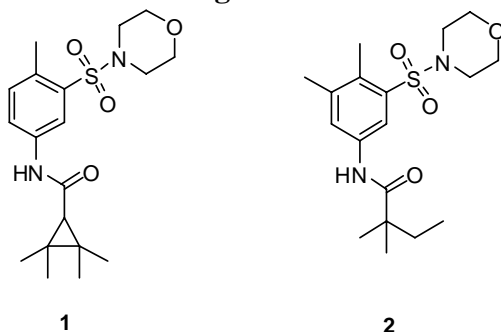
**“Novel Selective CB<sub>2</sub> Receptor ligands: Part VII – Indane and 1,2,3,4-Tetrahydronaphthalene aminosulfonamides”**

*Ian Sellitto, et al., Adolor Corporation*

The researchers at Adolor presented their work on selective cannabinoid receptor subtype 2 agonists (CB<sub>2</sub>). CB<sub>2</sub> receptors are mainly expressed in peripheral nerve terminals as

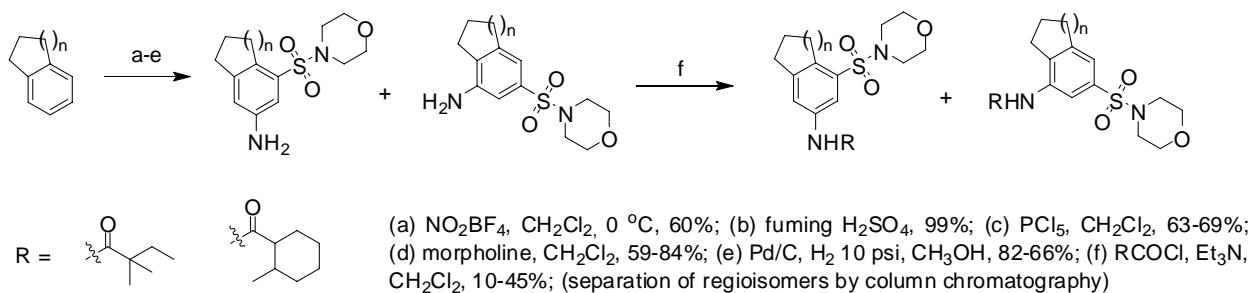
opposed to CB<sub>1</sub> receptors which are expressed mainly in the CNS. A selective CB<sub>2</sub> agonist could be useful for the treatment of pain without the undesired CNS effects (euphoria and altered memory) that are associated with CB<sub>1</sub> receptor activation. Previous work at Adolor had discovered aryl sulfonamide **1** (Figure 25) as a selective CB<sub>2</sub> agonist ( $K_i$  CB<sub>1</sub> = 3400 nM;  $K_i$  CB<sub>2</sub> = 23 nM). However, this compound had poor metabolic stability in rat and human liver microsomes and was only active *in vivo* when administered with a cytochrome P450 antagonist. Therefore, a new effort to improve the pharmacological profile of this series of compounds was begun using compound **2** ( $K_i$  CB<sub>1</sub> = 2500 nM;  $K_i$  CB<sub>2</sub> = 17 nM) as a starting point.

**Figure 25.**

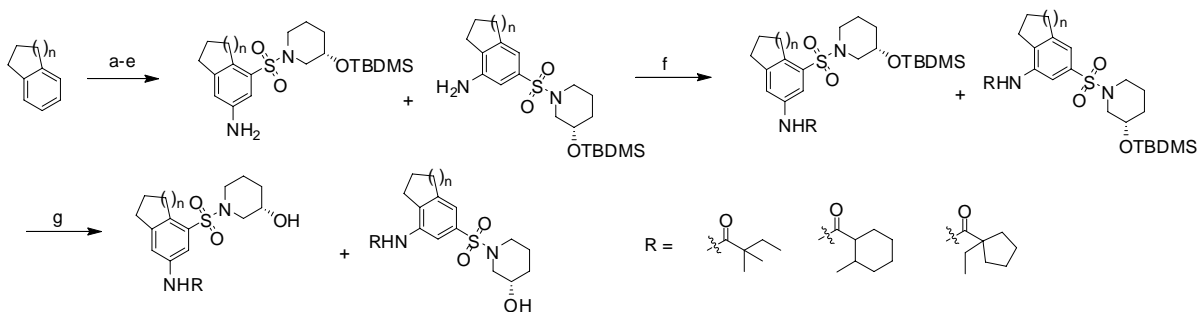


The synthetic routes used to prepare the target compounds are shown in Schemes 26 and 27. The compounds were synthesized as a mixture of regioisomers which were separated by column chromatography at the final step.

**Scheme 26.**



**Scheme 27.**



(a)  $\text{NO}_2\text{BF}_4$ ,  $\text{CH}_2\text{Cl}_2$ ,  $0^\circ\text{C}$ , 60%; (b) fuming  $\text{H}_2\text{SO}_4$ , 99%; (c)  $\text{PCl}_5$ ,  $\text{CH}_2\text{Cl}_2$ , 63-69%; (d) (S)-3-(TBDMSoxy)piperidine,  $\text{Et}_3\text{N}$ ,  $\text{CH}_2\text{Cl}_2$ , 40-61%; (e)  $\text{Pd/C}$ ,  $\text{H}_2$  10 psi,  $\text{CH}_3\text{OH}$ , 83-87%; (f)  $\text{RCOCl}$ ,  $\text{Et}_3\text{N}$ ,  $\text{CH}_2\text{Cl}_2$ , 40-80%; (g)  $\text{CH}_3\text{OH}$ , 4 M  $\text{HCl}$  in dioxane, 13-30% (separation of regioisomers by column chromatography)

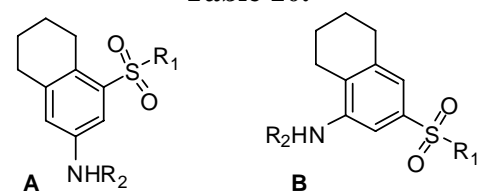
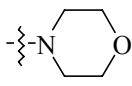
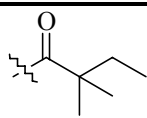
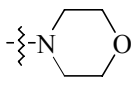
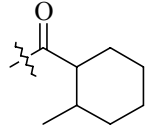
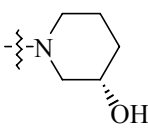
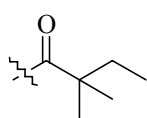
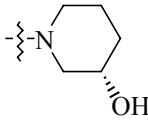
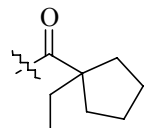
The  $\text{CB}_1$  and  $\text{CB}_2$  binding affinity for the 5 and 6 membered ring analogues is shown in Tables 9 and 10. As can be seen, the regioisomer A analogues consistently showed greater affinity for  $\text{CB}_2$  than the B isomer analogues.

**Table 9.**

Cmpd	R <sup>1</sup>	R <sup>2</sup>	Regio	Binding Affinity			
				K <sub>i</sub> CB <sub>1</sub> nM	K <sub>i</sub> CB <sub>2</sub> nM	K <sub>i</sub> Ratio CB <sub>1</sub> /CB <sub>2</sub>	CB <sub>2</sub> EC <sub>50</sub> nM
<b>3</b>			A	1700	12	140	28
			B	0.2%	1800	nd	nd
<b>4</b>			A	292	1.7	170	5.0
			B	1700	35	49	65
<b>5</b>			A	4600	7.1	650	11
			B	16%	510	nd	290
<b>6</b>			A	2200	1.4	1600	3.0
			B	16%	39	nd	50
<b>7</b>			A	3900	1.8	2200	4.3
			B	0%	99	nd	220

Replacing the morpholine group with a (S)-3-hydroxypiperidine was well tolerated and a variety of lipophilic groups could be installed at R<sub>2</sub> without significant loss of activity.

**Table 10.**

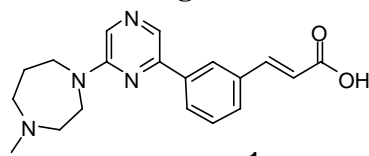
Cmpd	R <sup>1</sup>	R <sup>2</sup>	Regio				
				Ki CB <sub>1</sub> nM	Ki CB <sub>2</sub> nM	Ki Ratio CB <sub>1</sub> /CB <sub>2</sub>	CB <sub>2</sub> EC <sub>50</sub> nM
<b>8</b>			A	1400	14	100	47
			B	0%	49%	nd	nd
<b>9</b>			A	380	3.5	110	27
			B	17%	2100	nd	nd
<b>10</b>			A	40%	140	nd	185
			B	19%	3.6%	nd	nd
<b>11</b>			A	44%	33	nd	18
			B	9.4%	1900	nd	nd

Compound **5** was dosed in the hindpaw-incisional rodent model of postsurgical pain to assess its *in vivo* efficacy. At 30 mg/kg PO it was efficacious, but only for 15 min after dosing.

### “Hit to Lead Account of the Discovery of a New Class of Inhibitors of Pim-2 Kinase”

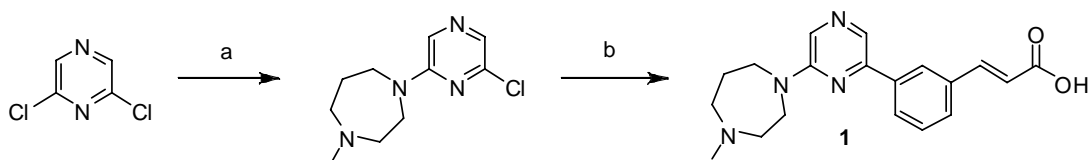
*Tina Morwick, Anthony Prokopowicz, Charles Cywin, Kevin Qian, Wang Mao, John, Wolak, Charlene Peng, Mohammed, Kashem, Jun Li, Lian Wang and Scott Jakes, Boehringer Ingelheim.*

Some work done at Boehringer Ingelheim has focused on investigating inhibitors of Pim-2 kinase. The Pim kinases are widely distributed with a high level of expression in hematopoietic tissue<sup>1</sup> and have been implicated as having a functional role in cell survival.<sup>2</sup> They have found that Pim-2 kinase expression is elevated in a variety of inflammatory states. One example is in patients with inflammatory bowel disease (IBD). Tissue samples taken from IBD patients show higher levels of Pim-2 kinase in inflamed tissue vs. non inflamed tissue. Therefore, it is thought that Pim-2 would be an interesting therapeutic target for inflammation. A screen of the company’s compound collection revealed compound **1** (Figure 26) to be a potent inhibitor of Pim-2 kinase.

**Figure 26.**

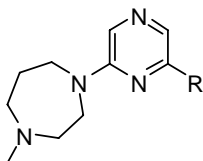
1  
IC<sub>50</sub> = 41 nM (Pim-2); 57 nM (Pim-1)

The general synthetic scheme for this class of compounds is shown below in Scheme 28. Studies were then undertaken to explore the SAR around this general scaffold.

**Scheme 28.**

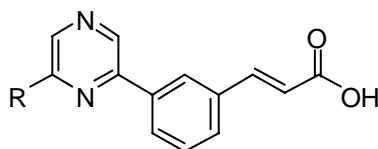
(a) N-methylhomopiperazine, CH<sub>2</sub>Cl<sub>2</sub>; (b) 3-(E-2-carboxovinyl)benzeneboronic acid, (PPh<sub>3</sub>)<sub>2</sub>PdCl<sub>2</sub>, 2M Na<sub>2</sub>CO<sub>3</sub>, DMF, microwave

As shown in Table 11, removal of the cinnamic acid side chain destroyed activity. Removal of the acid functionality was also not well tolerated. This region of the molecule proved to be highly sensitive to change and suggested that the acid was an important part of the pharmacophore.

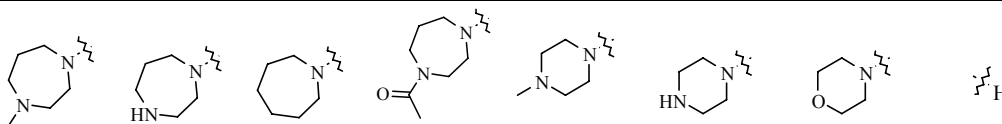
**Table 11.**

Compound	1	2	3	4	5	6	7
PIM-2 IC <sub>50</sub> (nM)	41	>5000	1200	>8000	1400	130	>16000

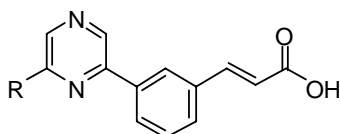
Table 12 shows some efforts at modifying the homopiperazine side chain. It was determined that the basic amine is necessary for activity as seen by the loss of activity going from compound 1 to compound 9. However, there did seem to be some tolerance in the placement and substitution of the amine.

**Table 12.**

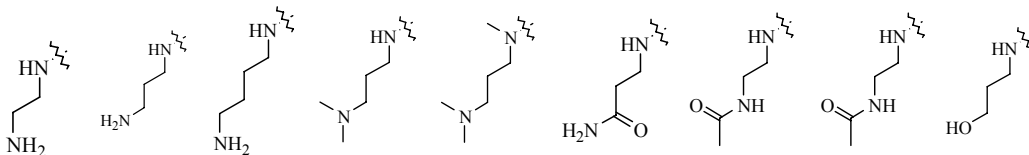
Compound	1	8	9	10	11	12	13	14
PIM-2 IC <sub>50</sub> (nM)	41	10	3300	880	150	200	1700	2200



Since there was some tolerance in changing the amine portion, further efforts were directed at opening the homopiperazine ring as shown in Table 13. In general, these compounds retained activity as long as a basic amine was present. Replacing the amine with an alcohol or ether resulted in a loss of potency.

**Table 13.**

Compound	15	16	17	18	19	20	21	22	23
PIM-2 IC <sub>50</sub> (nM)	140	27	22	94	370	250	1020	310	480



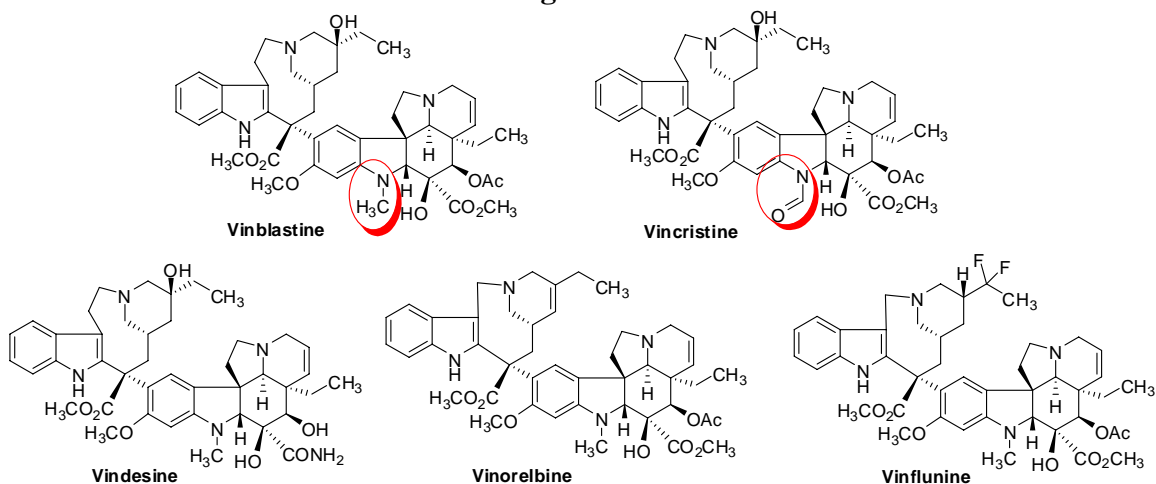
In conclusion, a new series of Pim-2 kinase inhibitors has been discovered. The presenters believed this was the first reported SAR study on inhibitors of Pim-2. For leading references on this work, see Mikkers, *et al.*, *Mol. Cell. Biol.* **2004**, *24*, 6104; Amaravadie, *et al.*, *J. Clin. Invest.* **2005**, *115*, 2618.

### “Synthesis and SAR of Novel 11’-Vinorelbine, 12’-Vinblastine, and 12’-Vincristine Alkaloid Analogues”

Matthew E. Voss, Jeffery M. Ralph, Dejian Xie, David D. Manning, Mark A. Wolf, Paolo Pasetto, Matthew D. Surman, Yeyu Cao, Thomas Friedrich, Denise Peace and Ian L. Scott, *Discovery R&D, AMRI, Albany, NY*

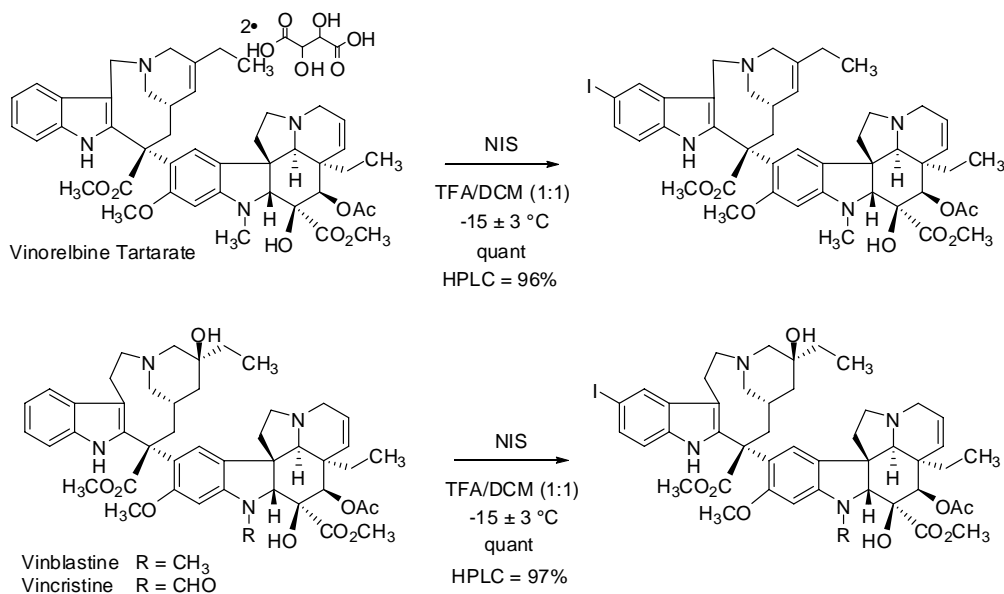
Voss gave a brief overview of Vinca alkaloid background. The structurally complex natural products inhibit tubulin formation through ligation to the tubulin monomers, and are thus used as treatments for cancer (Figure 27).

**Figure 27.**



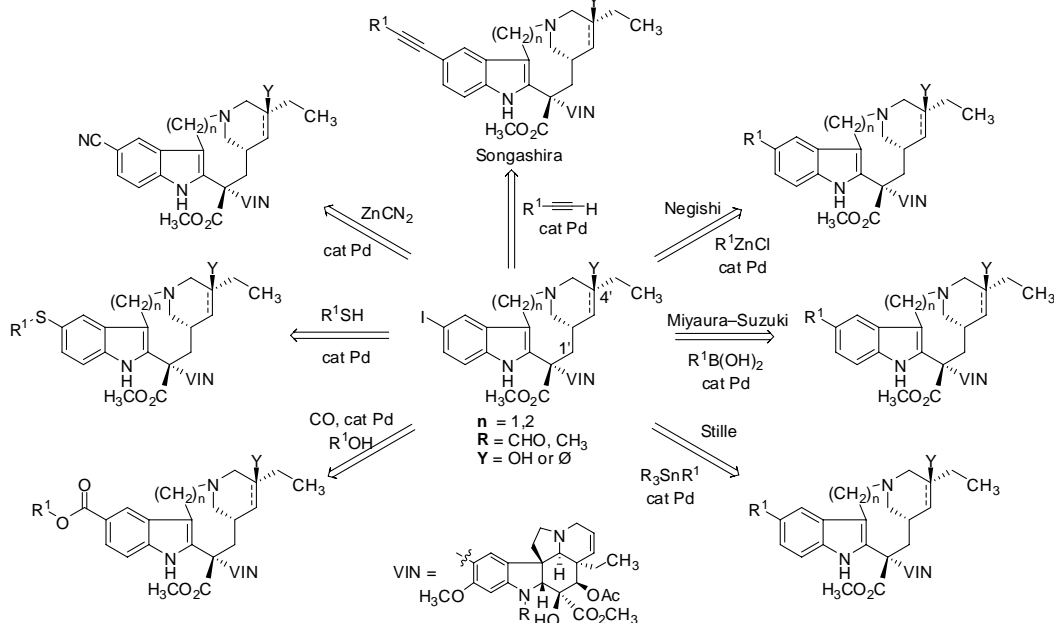
Small structural changes (Vinblastine to Vincristine) lead to drastic changes in clinical use and side-effect profile. Initial enzymatic work on the scaffolds showed a preference for halogenation at the 12' site. Based on this, AMRI initiated a search for scalable and selective halogenation conditions. The results of these efforts are shown in Scheme 29.

**Scheme 29.**



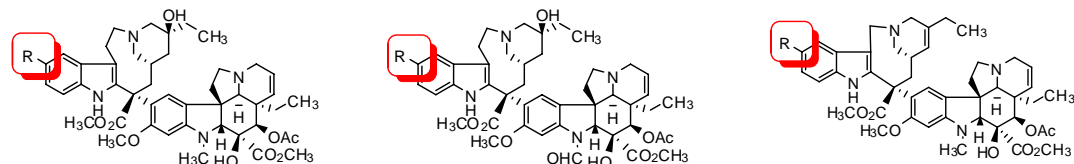
The utility of the 12'-iodide is shown in Figure 28.

**Figure 28.**



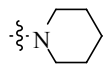
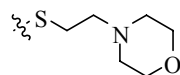
AMRI has utilized each of these pathways to produce novel Vinca-based derivatives with interesting *in vitro* biological activity as illustrated in Table 14.

**Table 14.**



<b>R</b>	MCF7 (nM)	HeLa (nM)	MCF7 (nM)	HeLa (nM)	MCF7 (nM)	HeLa (nM)
-H	0.4	0.9	1.5	1.7	2.4	2.7
Ph-	300	400	35	50	300	70
4-F-Ph-	95	250	300	500	-	-
4-OCH <sub>3</sub> -Ph-	125	200	400	200	-	-
2-thiazolyl-	100	200	-	-	-	-
2-thienyl-	300	300	-	-	-	-
-CHO	3	3	30	10	-	-
-COCH <sub>3</sub>	100	200	-	-	20	4
-CO <sub>2</sub> CH <sub>3</sub>	30	20	-	-	50	30
-CO <sub>2</sub> CH <sub>2</sub> CCl <sub>3</sub>	200	30	-	-	>1000	300
-CO <sub>2</sub> H	>1000	>1000	-	-	>1000	>1000
-CONH <sub>2</sub>	>1000	>1000	-	-	>1000	>1000
-CONH(CH <sub>3</sub> ) <sub>2</sub>			-	-	>1000	>1000

**Table 14 (continued).**

<b>R</b>	MCF7 (nM)	HeLa (nM)	MCF7 (nM)	HeLa (nM)	MCF7 (nM)	HeLa (nM)
-H	0.4	0.9	1.5	1.7	2.4	2.7
-OH	20	20	-	-	-	-
-SH	30	20	-	-	60	40
-NH <sub>2</sub>	200	200	-	-	600	300
-N(CH <sub>3</sub> ) <sub>2</sub>	50	30	-	-	-	-
	30	20	-	-	-	-
-CH <sub>2</sub> N(CH <sub>3</sub> ) <sub>2</sub>	>1000	>1000	-	-	-	-
<b>-SCH<sub>3</sub></b>	<b>2</b>	<b>0.6</b>	<b>3</b>	<b>3</b>	<b>1</b>	<b>0.3</b>
-SCH <sub>2</sub> CH <sub>3</sub>	3	2	8	6	20	5
-S(CH <sub>2</sub> ) <sub>2</sub> CH <sub>3</sub>	25	25	-	-	-	-
-SO <sub>2</sub> (CH <sub>2</sub> ) <sub>2</sub> CH <sub>3</sub>	>1000	500	-	-	-	-
-SCH <sub>2</sub> CO <sub>2</sub> H	200	50	-	-	-	-
	30	8	-	-	-	-
<b>-CH<sub>3</sub></b>	<b>0.3</b>	<b>0.3</b>	<b>3</b>	<b>1</b>	<b>50*</b>	<b>30*</b>
-CH <sub>3</sub>	0.3	0.3	3	1	50*	30*
-CH <sub>2</sub> CH <sub>3</sub>	0.6	0.3	10	5	-	-
-CN	3	3	4	10	6	1
-CCH	5	20	-	-	5	0.4
-(CH <sub>2</sub> ) <sub>5</sub> CH <sub>3</sub>	40	30	-	-	-	-

\*3-methoxy-11'-methylvinorelbine

The data in table 14 shows that a wide variety of functionalities are tolerated on all three Vinca-scaffolds in both MCF7 and HeLa assays. Small H-bond donors were not tolerated, however small alkyl groups and thioethers showed the most promising results. More importantly, the *in vivo* data for some of the substituted derivatives is significantly better than the natural product (Table 15), showing drastically increased post-treatment lifespans. In summary, AMRI has devised a clean and efficient route to substituted Vinca alkaloids and has shown, in some cases, greatly improved activities over the natural products.

**Table 15.**

Treatment Regimen (i.p., q4d × 3)		Median TTE <sup>a</sup>	% T/C <sup>b</sup>	Statistical Significance <sup>c</sup>
Compound	mg/kg			
Vehicle	-	21.0	---	---
Vinorelbine	12	24.5	117%	ne
	6	24.0	114%	ns
12'-Methyl	6	38.0	181%	***
Vinblastine	3	28.0	133%	**
12'-Thiomethyl	8	51.0	243%	***
Vinblastine	4	23.0	110%	ns
12'-Thiomethyl	4	26.0	124%	*
Vinorelbine	2	21.5	102%	ns
12'-Methyl	12	22.0	105%	ns
Vincristine	6	22.5	107%	ns

**Total Days of Study = 60;** <sup>a</sup>TTE – Time to Endpoint; <sup>b</sup>% T/C = (median TTE for treated animals)/(median TTE for untreated animals) × 100; <sup>c</sup>Statistical Significance = Logrank test: ne = not evaluable due to >10% mortality rate, ns = not significant, \* =  $P < 0.05$ , \*\* =  $P < 0.01$ , \*\*\* =  $P < 0.001$ , compared to vehicle control group

---

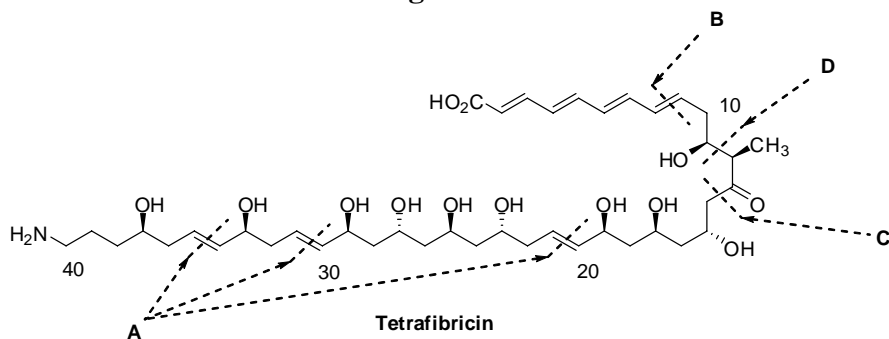
#### “Tetrafabricin: Synthesis of C1-C20 and C21-C40 fragments.”

Venugopal Gudipati\* and Dennis P. Curran, Department of Chemistry, University of Pittsburgh (\* Currently at AMRI, Albany, NY)

Tetrafabricin (Figure 29) is a potent fibrinogen receptor inhibitor, isolated from *Streptomyces neyagawaensis* (T. Kamiyama, *et al.*, *J. Antibiot.* **1993**, 46, 1039). The stereochemical structure was elucidated by Kishi and coworkers (Y. Kobayashi, *et al.*, *Org. Lett.* **2003**, 5, 93), and partial syntheses were reported by BouzBouz and Cossy (*Org. Lett.* **2004**, 6, 3469) and by Lira and Roush (*Org. Lett.* **2007**, 9, 533). The authors describe their attempts at a convergent total synthesis.

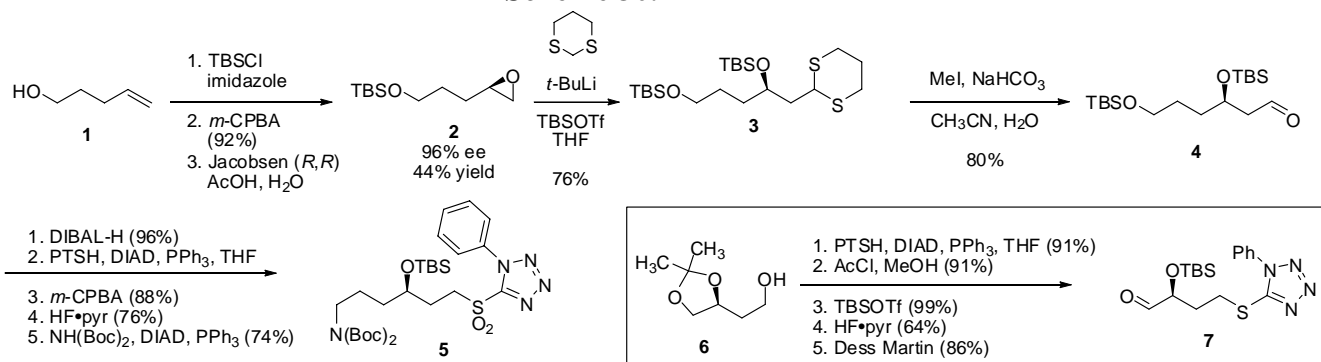
The planned disconnections are shown in Figure 29: the three *E* alkenes labeled **A** are selectively installed using a Kocienski-Julia olifenylation; the olefin marked **B** is formed using Horner-Emmons-Wadsworth chemistry; the bond labeled **C** is installed in an umpulung fashion *via* dithiane chemistry; and the bond labeled **D** is formed using an asymmetric aldol condensation.

**Figure 29.**



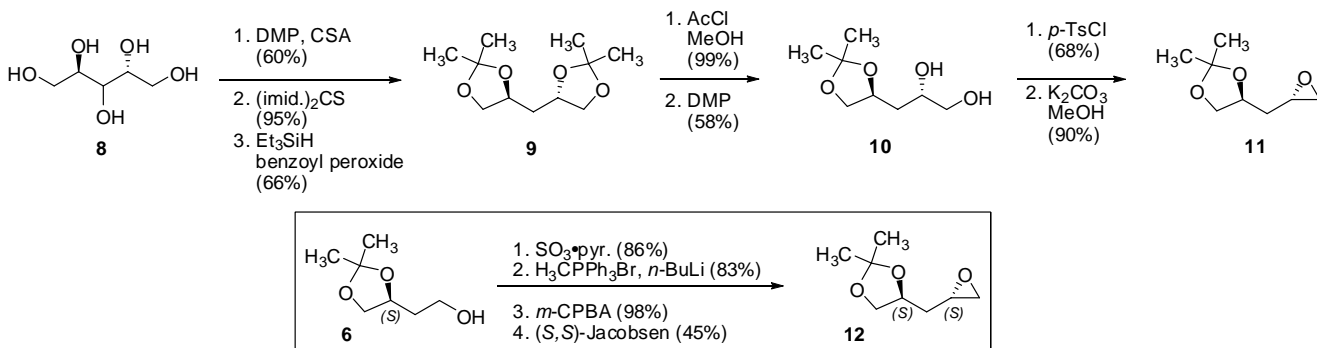
The synthesis begins with alcohol **1** undergoing protection and subsequent epoxidation and resolution to afford chiral epoxide **2** (Scheme 30). Homologation *via* dithiane chemistry is then performed in a 2-pot 3 step sequence to afford bis-protected diol **4**. The final Kocienski intermediate **5** was synthesized in five steps highlighted by two Mitsunobu reactions. In a similar fashion, acetonide **6** was converted to compound **7** in five steps. Oxidation of **7** was not performed to allow for selective olefination in a later step (*vide infra*).

**Scheme 30.**



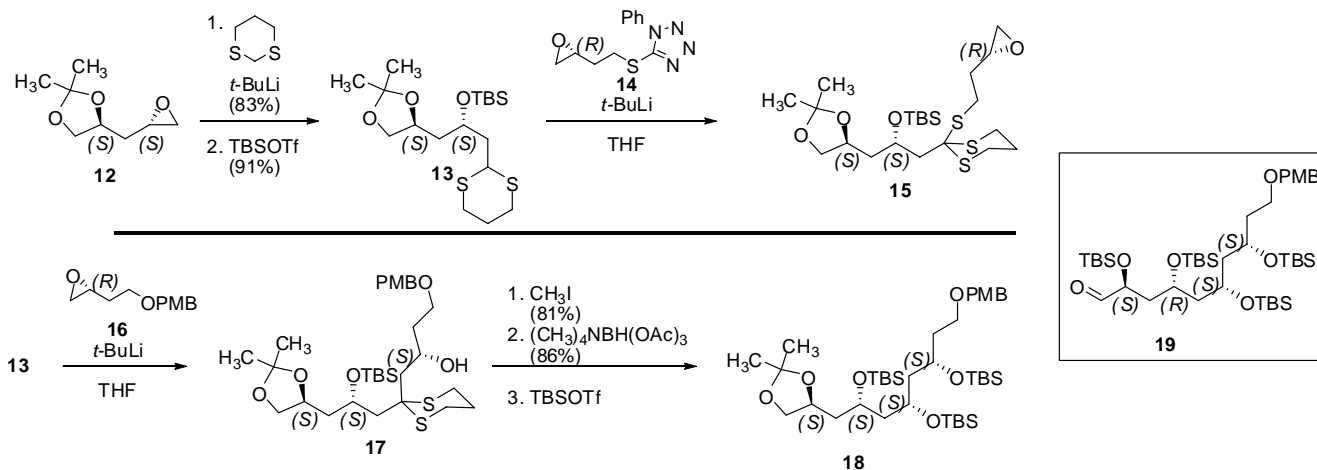
The first generation racemic synthesis of **11** is shown in Scheme 31. Conversion of arabitol **8** to its bis-acetonide, followed by a 2-step deoxygenation afforded compound **9**. A deprotection-reprotection sequence afforded the desired diol **10** in a fairly inefficient manner. Treatment of the diol with tosyl chloride followed by ring closure afforded compound **11**. A nice improvement to the procedure is also shown in Scheme 3. Commercially available alcohol **6** is oxidized followed by Wittig olefination. Alkene epoxidation followed by hydrolytic resolution afforded the desired (*S,S*) enantiomer (compound **12**) in 31% overall yield.

### Scheme 31.



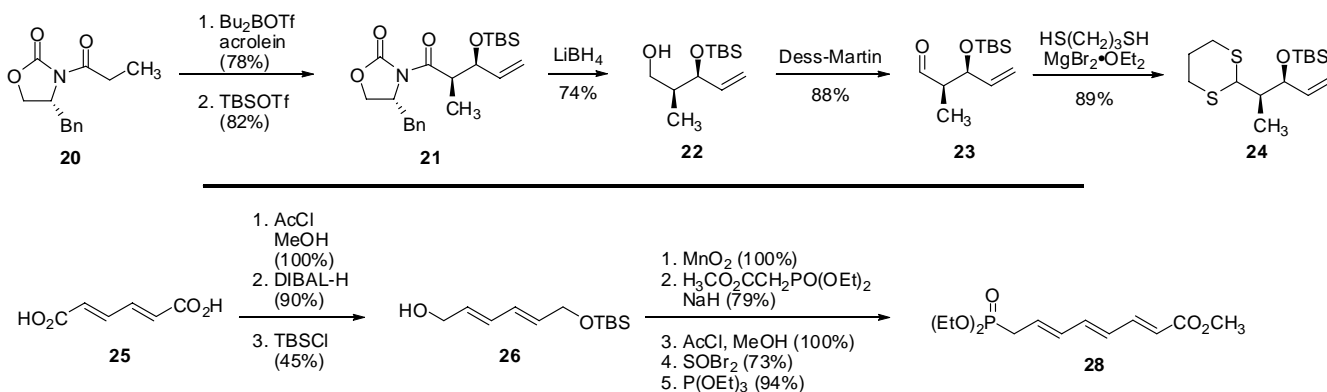
The homologation of compound **12** is shown in Scheme 32. Treatment of **12** with the dithiane anion afforded compound **13** after TBS protection. Unfortunately, treatment of the anion of **13** with **14** afforded **15**, derived from nucleophilic attack on sulfur. This result was confirmed in simple model systems (not shown). The result indicated that installation of the Kocienski functionality needed to be performed later in the sequence. To this end, compound **13** was reacted with epoxide **16** followed by deprotection, selective reduction and global silylation to afford key intermediate **18**. In work not described, the use of **18** in a late stage portion of the synthesis failed, requiring the synthesis of **19** using similar methodology.

### Scheme 32.



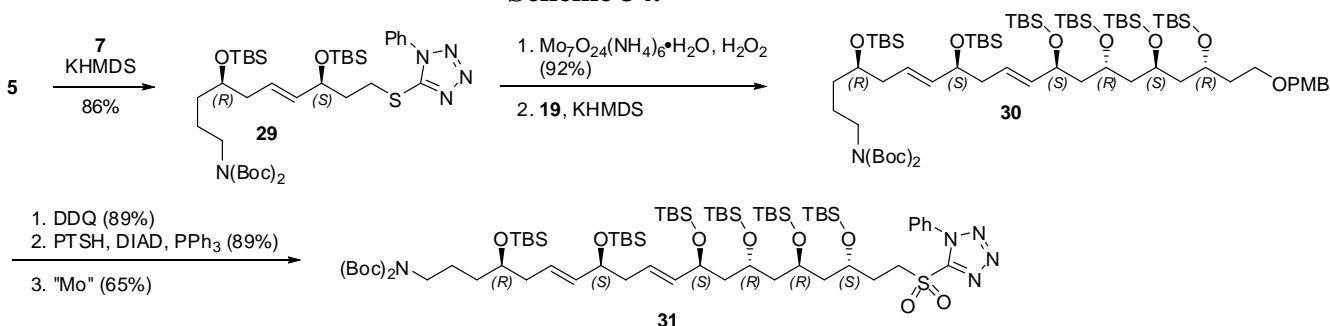
The synthesis of the final two fragments is shown in Scheme 33. Evan's precursor **20** is alkylated to give **21** stereoselectively. Removal of the chiral auxiliary followed by oxidation and dithiane formation afforded the intermediate **24**. Di-acid **25** can be esterified, reduced and mono-protected to afford **26**. Oxidation of **26**, followed by Horner Emmons Wadsworth homologation afforded the triene **27**. Acidic desilylation, bromination and phosphonation yielded compound **28**.

### Scheme 33.



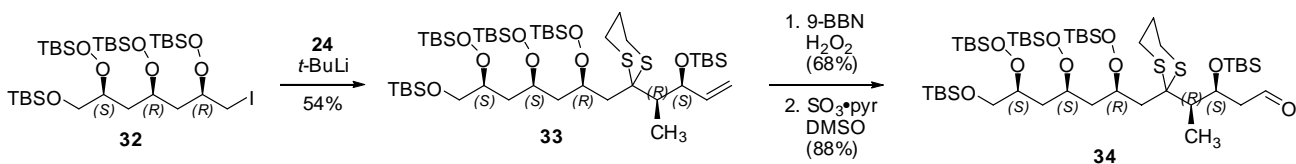
The condensation of **5** and **7** afforded alkene **29**, which was subsequently oxidized and again condensed with **19** to afford advanced intermediate **30** (Scheme 34). Removal of the PMB group followed by a final Kocienski-Julia intermediate sequence afforded compound **31**.

### Scheme 34.

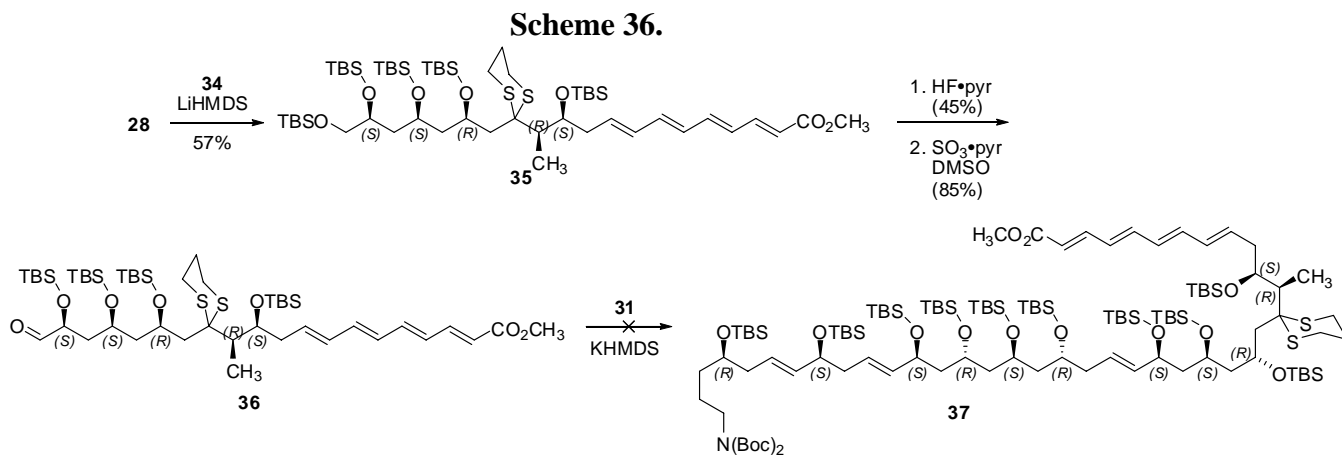


The deprotonation of dithiane **24** followed by treatment with **32** (synthesized in 9 steps using standard methodology, 32% overall yield) afforded alkene **33** (Scheme 35). Hydroboration-oxidation followed by further oxidation of the resulting alcohol afforded compound **34**.

### Scheme 35.



A Horner Emmons Wadsworth coupling between **28** and **34** afforded tetraene **35** which was selectively deprotected and oxidized to compound **36** (Scheme 36). Construction of the final scaffold **37** was unsuccessful. The author cited the limited material in hand and a re-synthesis is planned to complete the natural product.

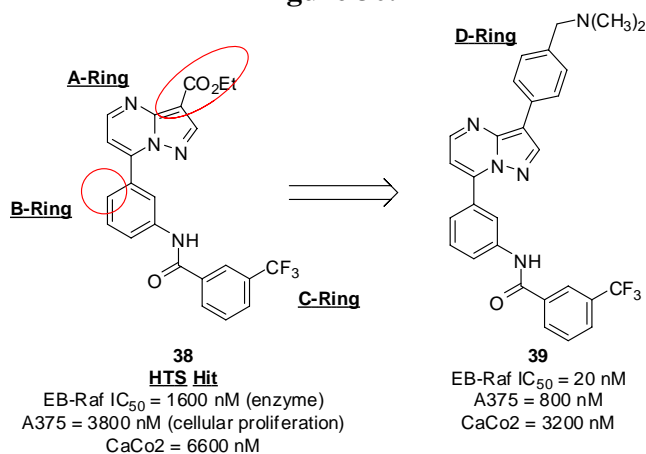


### “Synthesis and Activity of Pyrazolo[1,5-*a*]pyrimidines as B-Raf Inhibitors”

*Kyung-Hee Kim, et al., Chemical and Screening Sciences and Oncology Research, Wyeth Research, Pearl River, NY*

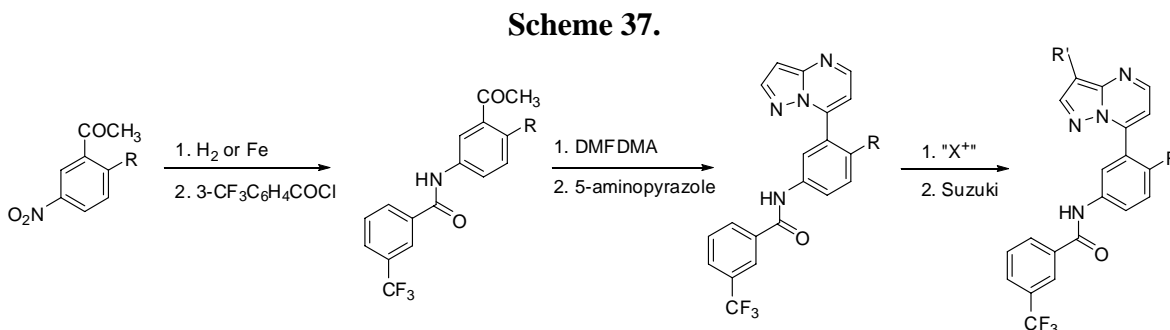
The poster presented described a portion of the work towards B-Raf inhibitors for the treatment of cancer. B-Raf is the key Raf Kinase in the signaling cascade resulting in cell growth. B-Raf mutations are prevalent in cancerous tumors and therefore inhibition of the enzyme represents a viable mechanism for tumor growth inhibition. The hit obtained from a library screen at Wyeth is shown in Figure 30 (compound **38**). Initial SAR led to the development of the dimethylaminomethyl compound **39** which displayed a marked improvement in activity. A crystal structure of **39** bound to the enzyme showed the basic amine interacting with the solvent, with no part of the molecule interacting with “hinge” portion of the receptor (kinase inhibitors often rely on hinge region interactions for activity).

**Figure 30.**



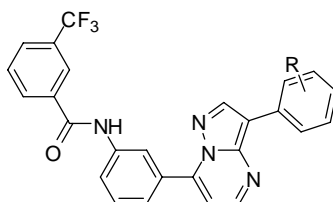
The synthesis of the B-Raf inhibitors is shown in Scheme 37. Various substituted 3'-nitroacetophenones are reduced and acylated. The resulting amides are homologated with

DMFDMA followed by cyclization with 5-aminopyrazole (substituted pyrazoles can be used in cases where a final Suzuki reaction is inappropriate). Selective halogenation of the resulting pyrazolopyrimidine is followed by a cross coupling reaction to complete the sequence.



The first set of SAR data is shown in Table 16. A variety of substituted phenyl derivatives were synthesized, with methanol functionalities showing an improvement in activity at the 3- and 4-positions.

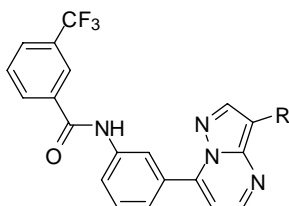
**Table 16.**



Cmpd	R	enzyme (nM)	cellular (nM)	Cmpd	R	enzyme (nM)	cellular (nM)
40	2-COCH <sub>3</sub>	260	nd	48	3-CO <sub>2</sub> CH <sub>3</sub>	1770	nd
41	2-CH(CH <sub>3</sub> )OH	290	4500	49	3-CO <sub>2</sub> H	520	nd
42	2-CN	7400	nd	50	4-CH <sub>2</sub> OH	80	nd
43	3-CH <sub>2</sub> OH	140	nd	51	4-CN	>10000	nd
44	3-CH(CH <sub>3</sub> )OH	200	8300	52	4-CO <sub>2</sub> CH <sub>3</sub>	2000	nd
45	3-COCH <sub>3</sub>	610	nd	53	4-COCH <sub>3</sub>	4200	nd
46	3-CN	>10000	nd	54	3,5-CHO	>10000	6500

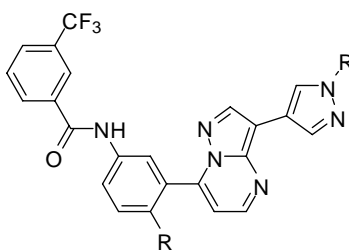
Heterocyclic replacements are shown in Table 17. Five-membered rings with a hydrogen bond donor showed the best activity. Modeling between pyrazole analogs and the crystal structure of the enzyme suggest an interaction between the pyrazole side chain and the hinge region. The carboxylate isostere (tetrazole compound **53**) showed no activity, possibly due to electrostatic repulsions with the aspartate and glutamate residues in the binding pocket.

**Table 17.**



Cmpd	R	enzyme (nM)	cellular (nM)	Cmpd	R	enzyme (nM)	cellular (nM)
40		130	560	48		80	nd
41		110	3240	49		2050	nd
42		590	nd	50		250	7000
43		>10000	nd	51		70	3900
44		120	2270	52		330	nd
45		940	670	53		>10000	nd
46		1330	2500	54		130	8100
47		850	1000				

Substitutions of the B-ring are shown in Table 18. Based on the pyrazole/hinge region interaction described above, the position on the B-ring labeled “R” should be aligned with a hydrophobic region of the binding pocket. To this end, compounds **55–60** were synthesized and showed good potency, but more importantly, improved activity in the cellular assay. Further studies showed that complete replacement of the D-ring with halogens, especially iodide afforded compounds with excellent potency. In conclusion, the authors reported SAR data that might be helpful in the plethora of ongoing kinase projects.

**Table 18.**

Cmpd	R (R' = H)	enzyme (nM)	cellular (nM)
55	F	20	420
56	Cl	40	210
57	OCH <sub>3</sub>	100	nd

Cmpd	R (R' = Boc)	enzyme (nM)	cellular (nM)
58	H	2050	nd
59	F	130	520
60	OCH <sub>3</sub>	320	nd